MHE 70LT

Ovchinnikov Ivan

Human gait modeling using MPC controller

MSc thesis

The author applies for

The academic degree

Master of Science in Mechatronics engineering

FOREWORD

This thesis is the final assessment paper of the double-degree program at Tallinn University of Technology and ITMO University (St. Petersburg). The main theme and field of work were chosen on the progress of dialogue among me and Professor Vu Trieu Minh. Writing the thesis took place at the Department of Mechatronics of Tallinn University of Technology.

I would like to thank to the two universities for the opportunity to get the great experience in the field of mechatronics and robotics and cooperation and orientation in another country with another language. And a special thanks to Department of Mechatronics of Tallinn University of Technology for providing the access to computer classes which have all the necessary software and hardware.

Special thanks I express to my supervisors Vu TM and Kovalenko PP for providing their knowledge and for help in choosing the direction of research and guiding. I would like to thank my lecturers Eduard Petlenkov for discussions about my research.

I would like to thank my parents and friends for their support during my study and research.

ABSTRACT

In this research are developed a model of human movement using prediction. The developed model includes a mathematical model of human gait, the model function as the control object and a control system in the form MPC, CNS mimics.

The effectiveness of the developed model is verified by simulation and comparison of the data with the experimental data. The simulation results showed that the model is able to predict the movement kinematics of a healthy person.

TABLE OF CONTENTS

1. INTRODUCTION

Gait of each person varies depending on the condition and its physical characteristics. Human gait includes simultaneous work of muscles, limbs and central nervous system (CNS). Therefore, despite the fact that most people have the general dynamics of movement, gait of each individual is unique. In recent years, a large number of models of orthoses and prostheses that mimic the human gait developed, but often their design and development is based mainly on intuition, followed by experimental verification. These approaches are costly, ineffective and unsustainable.

Considerable interest is the use of human gait simulation results in security systems for identifying people by their gait. By reading human gait and his mass with the help of cameras and weights room in the corridor, you can prevent an employee in a room with restricted access, such as a warehouse, deposit boxes, and so on, or block the entrance and / or exit to the offender, creating the appearance of a free access. Because such a system can be invisible and imperceptible to anyone, unlike the systems scan fingerprints, retina or face unlock, it speeds up the passage of employees in the right place, and in addition does not allow attackers to prepare for such a method of access control.

Modeling of gait and in medicine to detect various abnormalities and disorders of the musculoskeletal system is no less interesting. Since using the model doctors can check their assumptions about a disease or condition of the lower limbs without conducting experimentation on a patient.

Also modeling of human gait would greatly simplify the process of testing artificial limbs and orthotic devices, which are now checked empirically, despite the fact that this approach is expensive and ineffective.

This research aims to develop the most simple modular human gait simulation circuit which can be used to compare the simulation data and the data obtained by the motion capture cameras (Vicon) with the highest accuracy.

Recently, particular attention has been paid to modeling of human and anthropomorphic robots gait, as well as to issues related to the development and production of orthoses and prostheses for human lower limbs [1-3]. The question of the application of lower limb movement simulation results for identification of people by their gait, as well as for recognition of various deviations and disorders in the musculoskeletal system, is of considerable interest [4-5].

In the majority of papers devoted to modeling of the gait, Lagrange's equations and some limitations are used for describing movements of the limbs, as the position of a 5-link or 7-link mechanism cannot be described only by dynamics equations. For example, in [6] movement of center of masses undertakes such limiting condition. In this paper the good results which are almost matching the experimental data were received, however paths of movement of some points are absolutely incorrect, and the computing circuit is very difficult because of what it is possible to use it only for human gait simulation without violations. In [7, 8] limiting condition is a condition of minimization of energy, in [9] are starting and finishing points and simplification of dynamic equations. In papers [9, 10] only the analytical method of calculation is used, and in [6–8] the MPC controller is used. Papers in which influence of the upper extremities on dynamics of gait is considered [11] are also known.

Since human movement of is a complex work of muscles and the central nervous system, the problem of motion can be decomposed into three components: Analytical solution (estimated trajectory of motion), the calculation of the required signals to the muscles and muscle simulation work object. CNS performs first two problems at the person, human muscles directly perform the third task. In this research a mathematical model describing the path of movement of the anthropomorphic mechanism will be used for analytical solutions, which is close (but not sufficient) to the real. Model predictive control (MPC) will be used to solve the second problem, since it is assumed that a person walking trying to predict the future. 5-link model of the lower extremities (feet, shins, hips and body) will perform the third task. model movement will be carried out by the calculated controller torques.

The main goal of this work is the modeling of human gait. The principle of the central nervous system simulation using the MPC and the analytical calculation of the movement is taken for the control system simulation. For the development model used by the managed software package Matlab / Simulink.

2. LITERATURE REVIEW

Any study of gait simulation can be considered from two different points of view: From the point of view of the biomechanics of gait is a very difficult process because it uses a complex musculoskeletal model that can describe all the fine details of the human gait. The detailed impact of the muscles, tendons, ligaments, cartilage in the human gait is considered in detail in [2,12]. However, in such a biomechanical model is typically about one hundred degrees of mobility. Some of them may have a role in complicating consideration of human gait, because their effect may be low, or not to be, and every extra degree of freedom greatly increases the complexity of the system control. In addition, the current technology in the computing requires the use of supercomputers, which is unacceptable for the task. In terms of robotics model considerably simplified and dynamic model is simpler and solved under normal conditions. Therefore, this research selected approach to the description of gait in terms of robotics. Further analysis of the literature is divided into different categories of methods of investigation and management of such anthropomorphic models.

2.1.1. Inverted pendulum model

Gait is a transfer of kinetic and potential energies during the motion of center of mass in space. On the basis of this concept inverted pendulum is the most simple approximation gait dynamics. This method uses a model of a mathematical pendulum with a concentrated mass of a body at the center of gravity. It is usually assumed that the height of the center of gravity during movement does not change. With this statement the trajectory are calculated.

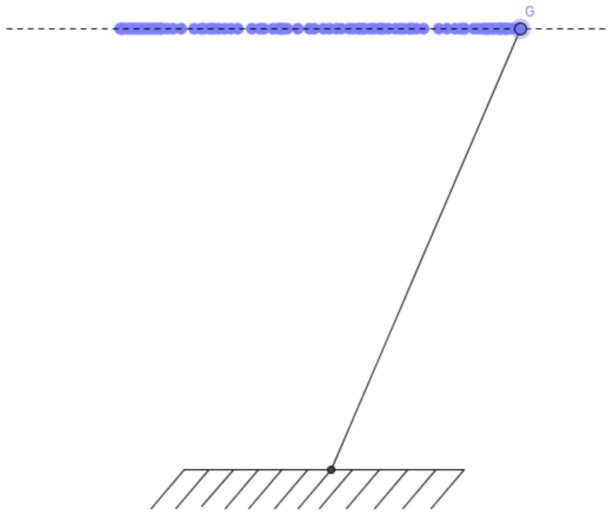

Figure 2.1: Inverted Pendulum

Inverted pendulum model commonly used to simulate the movement of human gait. In these models, the inverted pendulum in the plane considered. It consists of a weightless rod with variable length and mass concentrated at the end of the rod. Kajita et al. were the first to use an inverted pendulum, to simulate the gait, as they moved from the planar interpretation of 3D model to the same concepts [13,14]. Kudoh and Komura [15] improved this model by considering the angular momentum around the COG. Albert and Gerth [16] studied the dynamics of the site fluctuations and offered an inverted pendulum model with two masses. It is also worth mentioning Ha and Choi [17] where the COG height varies and is calculated by the method of the zero point, this method will be discussed later.

The main advantage of this method is the simplicity of modeling. However, with such a model cannot say anything about the dynamics of motion of joints, as they are not in the model. Passive Dynamic Walker is the next step in the development of gait simulation.

2.1.2. Passive Dynamic Walker

The model is based on the idea that such downtime biped model may come down with a slight incline without any external control or actuation, that is, alone (Fig. 1.2). This model is moving as a pendulum.

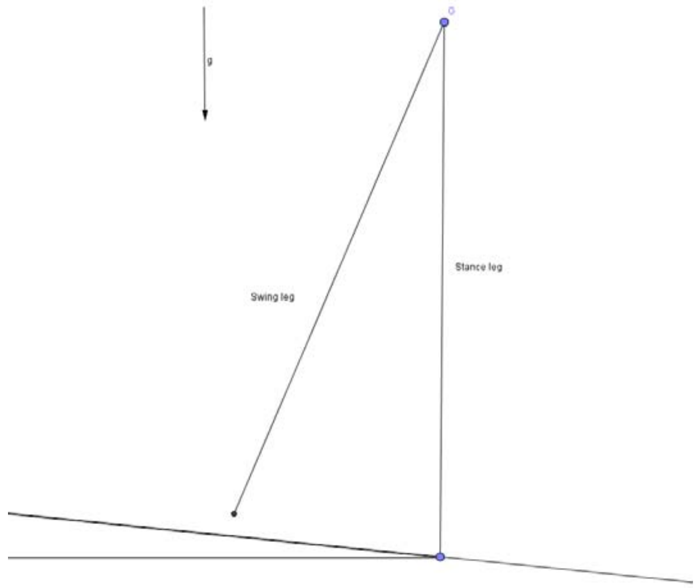

Figure 1.2: Passive Dynamic Walker

McGeer the first to describe this approach, it is suggested that the concept and led the governing equations in [18]. In addition, a prototype model of knee was successfully created to test the concept. Hurmuzlu in their work [19] further added to this model, the fifth link - the upper part of the body. Thus the influence of the upper body during the descent was examined. Springs and dampers were further added to this model to generate different versions of gaits. Next, Kuo [20] extended this model with the plane space, making it possible to tilt the model across (which corresponds to the inclination of the human hip in turn). This model can only go down the inclined surface so Collins et al. [21] added small actuators to compensate the loss of gravity.

The gait model proposed in this approach, a simple and energy-efficient and can provide some insight into the principles of human walking [22-24]. The drawback to this method is the same as a simple inverted pendulum model; This method does not simulate real movements of the joints, to generate realistic gait must take into account the dynamics and kinematics of the motion units, while the movement of the human body is given not only by gravity but also the internal forces in the system. Therefore it is necessary to use a more complex model for the simulation.

2.1.3. Zero-Moment-Point Method

The method of zero moment point (ZMP) is the idea of generating a two-legged gait, while respecting the balance of the human body using a number of predefined positions ZMP. The main objective here is not to coordinate all of gait as a whole, and guaranteed the stability of the body, i.e., for all states active the resultant torque forces is zero as shown in Fig. 1.3.

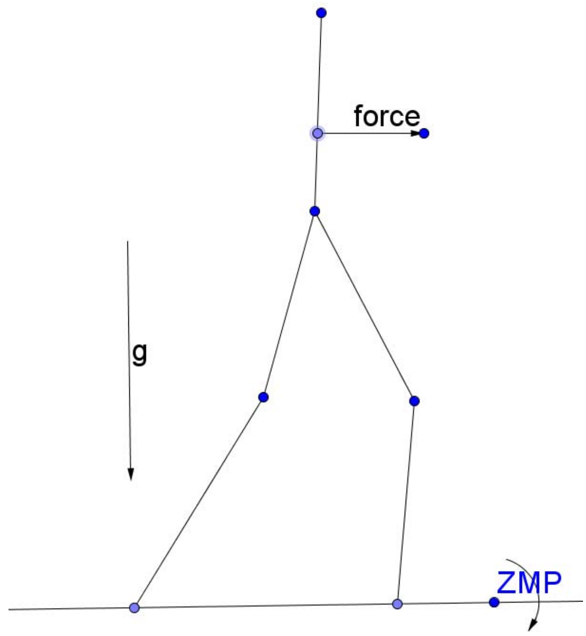

Figure 2.3: ZMP method

As a result, active powers can be managed so that the ZMP in the range of predefined positions and the center of pressure has always been on the contact surface of the legs and the floor.

The first application of the method ZMP belong Takanishi et al. [25] and Yamaguchi et al. [26], where a two-legged robot successfully bipedal gait. This approach is widely used to control the robot gait [27-28]. Hirai et al. [29] presented the development of a humanoid robot Honda, which had 26 DOFs, using ZMP method, as well as the Shih [30] proposed ZMP method to generate and control the movement of the robot with 7 DOFs.

The advantages of this method is that it is simple computationally, so it is so widespread in robotics, there are many studies in which controls the robot with 10+ DOFs successful, because for them it is important first and foremost, not a human resistance movement, and any stable bipedal movement. What precisely is the first disadvantage of this method, the motion described by this method is far from the human, although it is a biped. Another minus of this system is that the control system is very simple and devoid of optimization, as well as do not like the fact, how the human central nervous system, so it is worth considering further methods based on optimization of the movement.

2.1.4. Optimization-Based Method

In contrast to the inverted pendulum model, which focuses on the dynamics of human gait and ZMP method, which focuses on stability, optimization method is based on asking what criteria are used to generate the human central nervous gait. The problem of optimization can be summarized as follows:

$$\text{Find x} \tag{2.1}$$

$$\text{Minimize f(x)} \tag{2.2}$$

$$\text{subject to } g_i(x) \le 0, \text{and } h_j\,(x) = 0 \tag{2.3}$$

where $f(x)$ has the objective function, which, $g_i(x)$ and $h_j\,(x)$ restrictions must be minimized. Most often, for the variables (x) adopted a total time of each connection. The objective function $f(x)$, used in the analysis of gait usually function system performance measures. Limitations associated with the limitations of gait, as people are not able to turn the body on certain angles, as well as efforts in the compound as limited capacity of muscles. Once optimal x are obtained, they are substituted into the dynamic model for gait creation gait end. Dynamic model gait is often simplified to a rigid link model that has five or more degrees of freedom. According to [31], the governing equations of motion (EOM), to introduce the mechanics of the human gait are usually written in the form:

$$M(z) \cdot \ddot{z} + C(\dot{z}, z) + G(z) = \tau(t) \tag{2.4}$$

Where z rotation angles units, $M(z)$ inertia matrix, $C(\dot{z}, z)$ matrix of Coriolis and centrifugal force, $G(z)$ is the force of gravity and external force, τ have joint moments and t is time.
Depending on how the fit to eq. 2.4, there are two ways for the gait modeling: inverse dynamics or forward dynamics. The inverse dynamics approach calculated forces and

moments from the pilot position, velocity and acceleration, that is, the movement of the body [26]. These forces can then be used in the model for its movement. The approach is computationally efficient because EOMs are not integrated in the solution process. However, in this decision there is no feedback that the person provides the central nervous system, so this method is certainly not lead to the desired result. With the CNS, people are able to adjust the torques of each unit, and thus cause the system to the desired position.

Another way of computing it forward dynamics approach calculates the movement of the predetermined forces and moments by integrating the left side of the equation 2.4 with the given initial conditions, which means that this method is difficult to calculate. To optimize the forward dynamics, forces are variable. The movement is obtained by integrating the EOMs with initial conditions. The optimum gait is determined by minimizing an objective function. Unlike inverse dynamics, the advantage of this approach is that it essentially simulates the gait of human control.

Various performance indicators are already being used in a method based on optimization. The most commonly used performance indicators are described in [31]:

Stability:

$$\mathrm{f} = \int_0^T S dt \tag{2.5}$$

Where S is a measure of the stability of a particular method is usually above ZMP.

Metabolic energy:

$$\mathrm{f} = \int_0^T \dot{E} dt \tag{2.6}$$

Here metabolic energy expended by the body is reduced to a minimum. Metabolic energy allows for the mechanical energy, as well as other attendant energy losses, such as heat.

Mechanical energy:

$$\mathrm{f} = \int_0^T \tau \cdot \dot{z} dt \tag{2.7}$$

Minimizing the loss of mechanical energy.

Jerk:

$$\mathrm{f} = \int_0^T \dot{\tau} \cdot \dot{\tau} dt \tag{2.5}$$

Minimizing changes torques in joints

Dynamic effort:

$$\mathrm{f} = \int_0^T \tau \cdot \tau dt \qquad (2.5)$$

Dynamic force and mechanical energy measures are most often used in modeling the robot gait [32]. Metabolic rate performance, as a rule, used in biomechanical gait analysis [33]. In fact, human gait may be determined by several measures the effectiveness of functioning together. Some researchers have conducted studies into the optimum combination of target functions, which are discussed in detail in [34].

The main advantage of this method is that it gives some idea of the principles of human gait using various performance measures. Furthermore, this method is able to handle large DOF model, which means that it can be used on complex models of the human gait. The disadvantage of this method is that it requires a lot of calculations thus it is not suitable for the development model, which pays a minimum time for simulation and calculation. In addition the method requires a function, which in some cases is extremely difficult to obtain, for example for pathological gaits, where just the action of these functions in the central nervous system can be violated, as people can not consciously adhere to minimize energy consumption, hence the CNS, should be guided by another control method gait.

*2.1.5. **Pulse method for controlling anthropomorphic mechanisms***

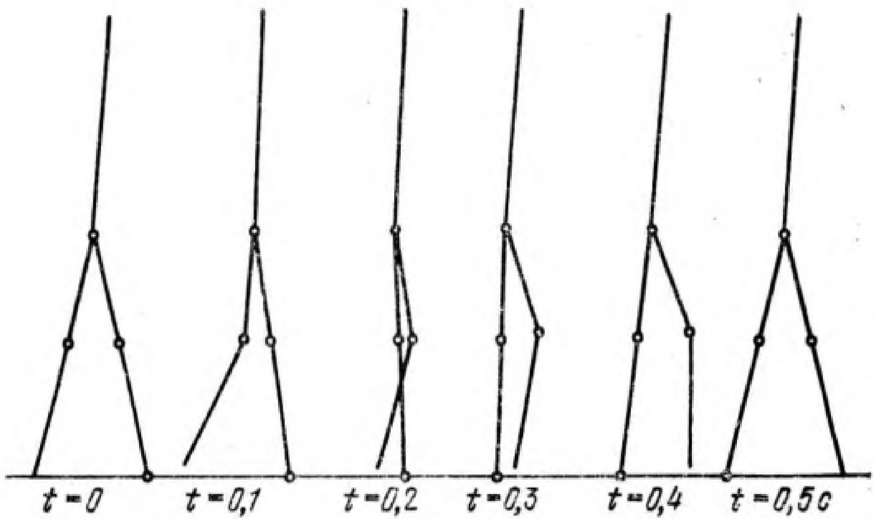

Figure 2.4: Impulse method

The basic idea of the pulse method is that the movement of n-tier anthropomorphic mechanism occurs on ballistic trajectories. The trajectory of motion of the system is achieved with a known initial (A) and end (B) of the provisions, due to the initial calculation of the necessary pulse system to independently come from position A to position B. This method is similar to the Passive Dynamic Walker, however, has a more complex structure, and the initial force. In [9 - 10] the results are close to the human gaits were obtained. However, since taken into account only the mass, length units such movements purely mechanical or analysis that is more like the part of the central nervous system, which calculates the approximate path, without taking into account the state of the muscles, by which the movement is given by a person. Split-second movement is shown in Fig. 2.4.

2.1.6. Control Based Methods

Control Based Methods are closer to modeling the human central nervous system than the previous ones, as well as the most common in the theory of control mechanisms and other systems. Systems controlled by Control Based Methods, can respond to change and interact with the environment, and to perform certain tasks in real time. The best known method is to use the PID controller, widely used in industry, but this method is based on the accounting system error that occurred with the help of the feedback, that the already mentioned reasons, cannot be applied to the problem of this paper. CNS predicts straight on the road, what will happen in the future, and on this basis adjusts effort in the system [35]. However, in this method, there are other controllers. Hurmuzlu et al. [19] studied the various control methods for gait simulation.

Among the control based methods as there are currently used to simulate the gait optimal control method. In optimal control method, the input joint moments are unknowns in the EOMs and are continuously optimized for the next time step with the kinematic feedback provided.

2.1.7. MPC

One such optimal control method is a model predictive control (MPC). MPC is based on an iterative, finite horizon optimization of the motion. One sub-area of the optimal control is called model predictive control (MPC). MPC is based on an iterative, finite horizon optimization of the motion. In this approach, the current state of the gait is discretized at time t to minimize a cost function for the optimal trajectory over a relatively short period of time in the future: [t, t + tN], where tN represents the final time. Specifically, state trajectories are explored which emanate from the current state and find a control solution which can minimize a cost function up to time [t + tN]. This optimization problem is repeated starting from the current state, yielding a new control and a new predicted state path. The futures states which are predicted keep shifting for the next time step.

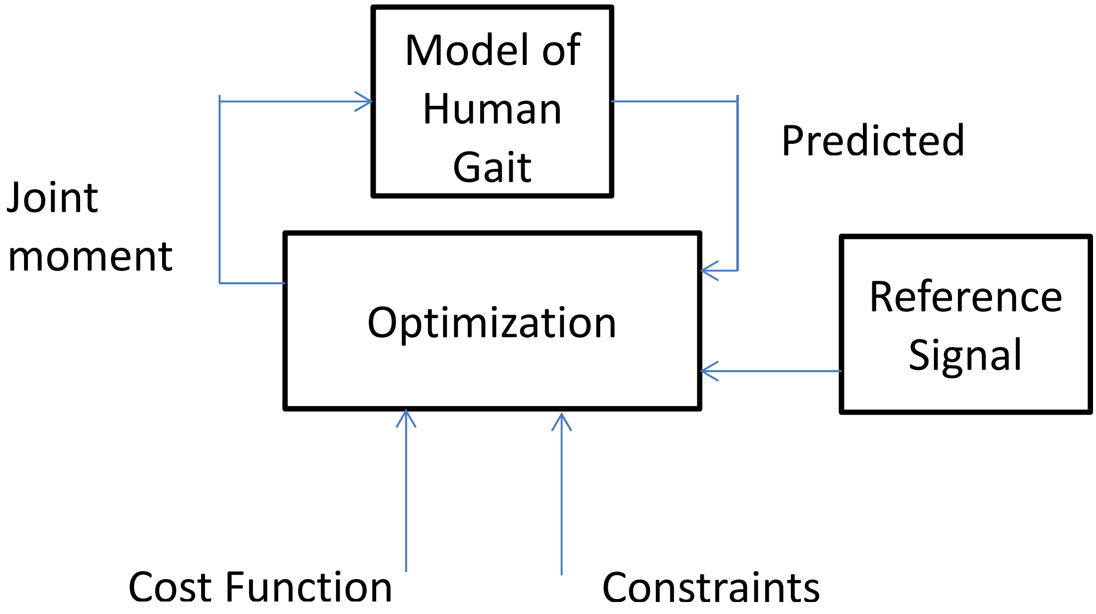

Figure 2.5: Block diagram of system controlled by MPC

The block diagram of system controlled by MPC applied to human gait analysis is shown in Fig. 2.5. A number of researchers have applied MPC method to simulate the central nervous system in the study of human gait. . Kooij et al [35] was developed predictive control algorithm in which only three parameters are selected as control targets: step time, stride length and velocity of the center of mass of repulsion. By using a seven-link eight DOF dynamics model and re-linearizing this model at each time interval, repetitive gait was reportedly generated. [36] utilized a similar seven-segment model as the plant with MPC as the control algorithm to simulate level walking. Different from Kooij et al. [35], the minimization of mechanical energy expenditure was employed as the major cost function. The references for the predictive control are also different, namely walking velocity, cycle period and double stance phase duration. Although repetitive walking was not generated, a complete cycle of human gait was successfully simulated. Their conclusion shows that minimizing energy expenditure should be the primary control object.

Other performance objectives have also been incorporated to improve simulation results. Gawthrop et al. [36] compared the predictive control method and the non-predictive control method, i.e., typical feedback PID control, to control a inverted pendulum. Results showed that the predictive control provides a better simulation than the traditional feedback control in that the time-delay is smaller. However, this work was not extended to full dynamic human gait model and its main concentration was on the balancing of the inverted pendulum. Karimian et al. [37] used MPC to control joint impedances of a 3D five-segment gait model.

The cost function of the controller was energy consumption, vertical orientation of the body, and forward velocity of the center of mass. Results showed that the model was able to achieve level walking, stairs ascent and descent.

2.1.8. Summary

Review of the literature shows that for human gait modeling the most potential control algorithm at the moment is to use the MPC, as the principal. Thus, MRS will be used as the main control algorithm of the model developed in this work. However, also with a good hand, it has proved to pulse control method.

3. DESIGN OF PLANT MODEL

There are three main objectives of the study: the first - to develop a model that with a certain accuracy to represent the dynamics of human movement, and the second - to develop an algorithm for calculating the approximate trajectory of movement of the mechanism, and the third - to implement the algorithm of predictive control system. This chapter focuses on the first purpose of the study.

In determining a model, we must first determine the desired level of accuracy. For the purposes of this study it is necessary that the model was a simple anthropomorphic mechanism to get a rough idea about the position of some points of the knee, lower leg, thigh and foot desirable, links angles of rotation, as well as a torque in the joints. From a management point of view, the model movement should occur by controlling the angles of links by changing torque. Such a process will approximately repeat the work of the CNS, in the form of feeding signals to the muscles that create a certain torque. So is it will limit the maximum and minimum points are not typical of the person, or his particular state, such as violations of the muscles or nerves.

The result was a 5-link mechanism to parameterize the model with seven degrees of freedom, taking into account the initial and final positions as well as the weight and length and step time units, such movement of can generate human gait.

3.1. Structure of the Plant Model

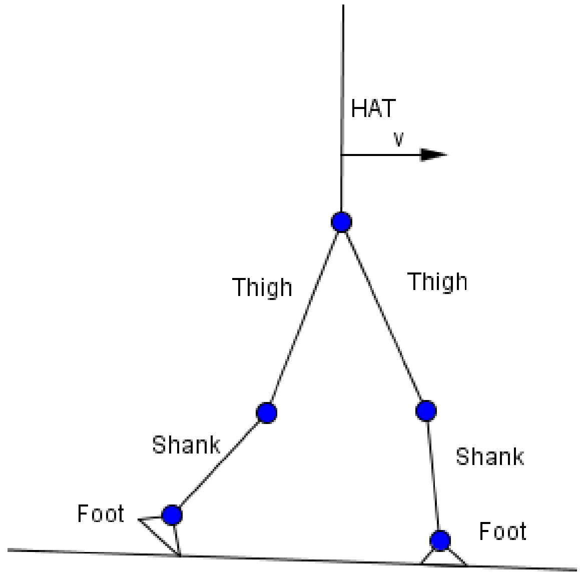

Figure 3.1: Seven link Gait model

As shown in fig. 3.1, the model can be developed by the seven links and nine degrees of freedom (DOF). The main five segments are shin, thigh on each side and a hard shell, which replaces the human body above the waist. The same pair of stop - two further segments can be added to the system. This simplification of the model to 5-link mechanism is taken since movement of foot has little effect on the general movement of the low weight, and the calculation of the foot rotation considerably complicates system.

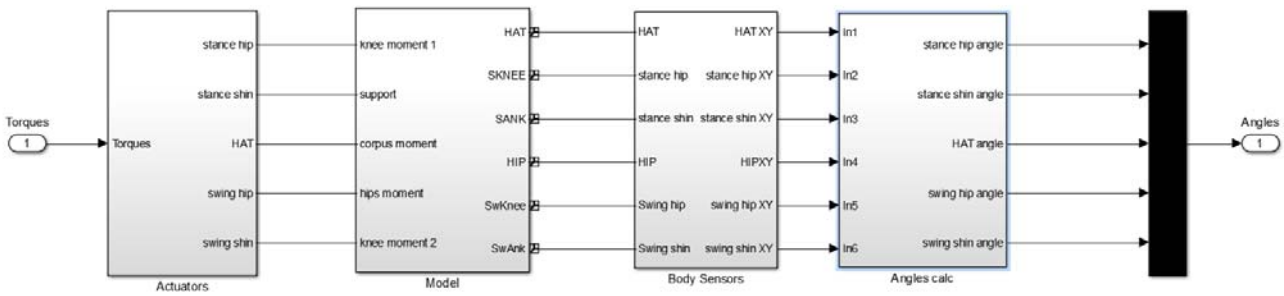

Figure 32.2: Plant in Simulink

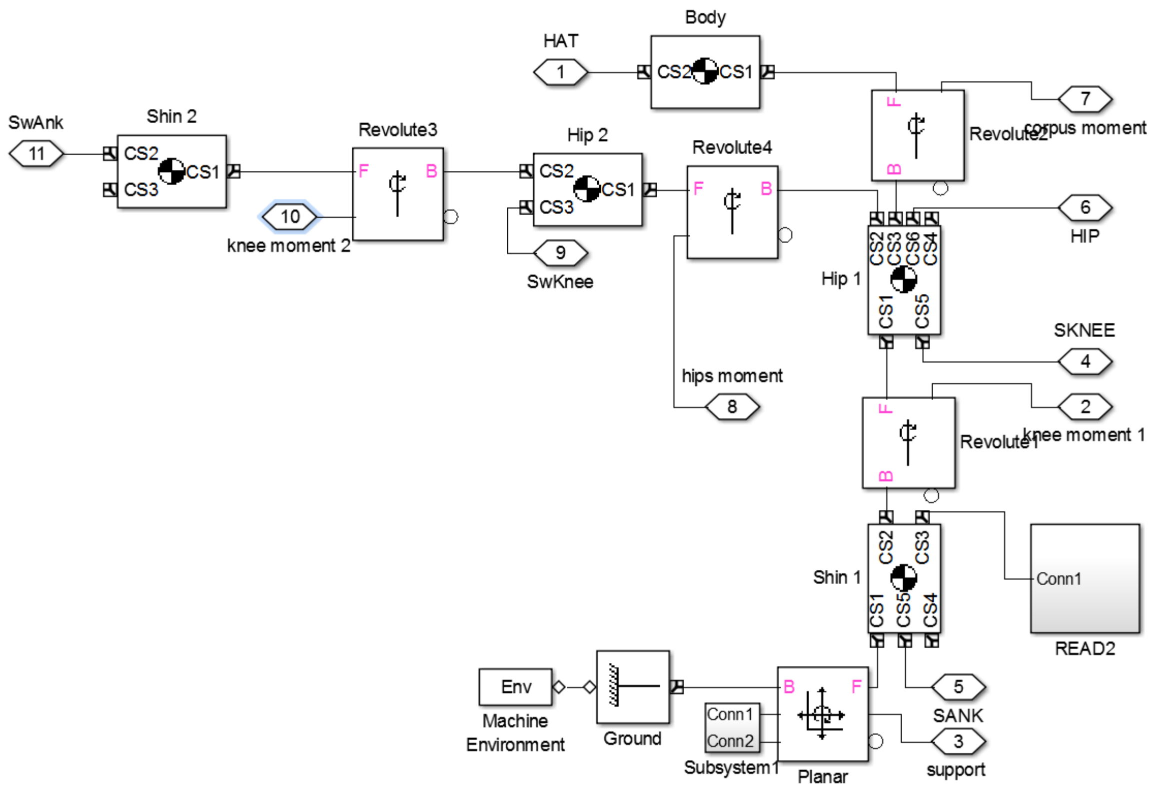

Figure 3.3: Model block in Simulink

Plant model developed in Matlab/Simulink (fig. 3.2). The inputs of the model are torques which are supplied to actuators to set the rotation of Model block links. Model block (fig 3.3) have 5 bodies connected to each other through 4 rotational connections, also model block have 6 outputs, which are transmit the position of connections in world coordinates. ‘’Angles calculation block’’ calculate rotation angles, there are variables that uniquely identify position of the model. This model describes the movement in one plane only. This simplification is permissible since movement in other planes significantly less [18]. Also, this model does not describe the movement of true human limbs, which also is a valid simplification [18].

4. MATHEMATICAL MODEL

Following the development of plant model, are two more parts of the study: The controller and the mathematical model that calculates the desired trajectory. This chapter explains the derivation of equations, which will be used as a reference for the MPC controller. Some intermediate equation calculated in [18], but they should be mentioned in order to prove the possibility of their use in this work.

4.1. General form

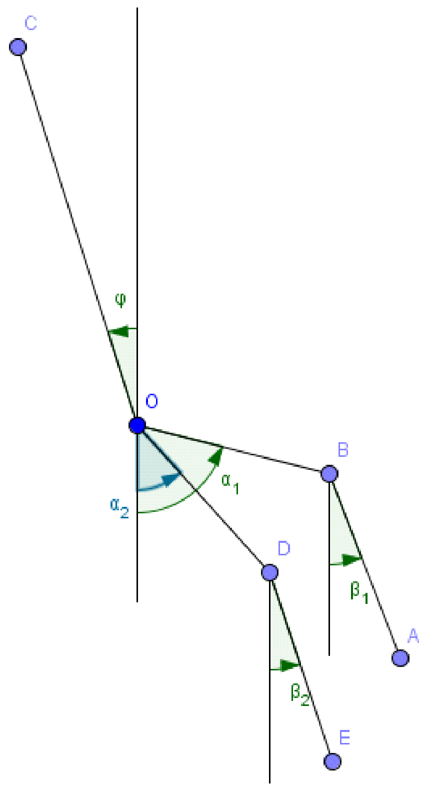

Figure 4.2: Five link Gait model

Fig. 4.2 shows a flat mechanism consisting of five weighty links OC, OB, OD, DE, BA. Link OC will be called the body, ODE and OBA - feet. Each leg consists of the thigh and lower leg, so that the links OB and OD are hips and units BA and DE are shins. Legs will be considered the same.

Joint O connecting the body OC with hips OB and OD will be referred as hip joint, joints B and D, connecting the thigh OB and OD with shins BA and DE, will be referred as knee joints. All joints are assumed to be ideal, i.e. friction in their neglect. This mechanism has seven degrees of freedom. In describing the situation as a six generalized coordinates, we choose the following works [39-41]: coordinates x, y of hip O and five angles ψ, α_1, α_2, β_1, β_2, between the links and the vertical. These angles and directions of their reference are shown in Fig. 2.2: ψ – the angle between the body and the vertical, α_1 и β_1 – the angles between the hips and the vertical, β_1, и β_2, – the angles formed by the vertical tibia. The angle is positive when the relevant unit deviates from the vertical direction in the opposite clockwise direction.

For this modeling simplified version of 5-link model used (human feet have a small part of all mass, and we may assume that feet do not have a strong influence on the movement of other parts of human).

Since the following equations are used directly in the system, it is necessary to describe the method of calculating.

4.2. The kinetic and potential energy of the system

Driving dynamics can be described by the Lagrange equation:

$$\frac{d}{dt} \cdot \frac{\partial L}{\partial \dot{q}_i} - \frac{\partial L}{\partial q_i} = Q_s \tag{4.1}$$

where Q_s – generalizes non conservative force.

$$L = T - V \tag{4.2}$$

where L – Lagrangian;

T – kinetic energy;

V – potential energy;

For kinetic energy:

$$T = \frac{1}{2}(m \cdot v^2 + 2 \cdot m \cdot (\nu \times \omega) \cdot p + \Theta \cdot \omega^2) \tag{4.3}$$

where m – mass of link;

v – absolute velocity;

ν – pole velocity;

ω – angular velocity;

p – radius vector of the center of mass;

Θ – Inertia moment relative to pole;

$$\nu = \begin{pmatrix} \dot{x} \\ \dot{y} \\ 0 \end{pmatrix} \tag{4.4}$$

$$\omega = \dot{\psi} \cdot \begin{pmatrix} sin(\psi) \\ cos(\psi) \\ 0 \end{pmatrix} \tag{4.5}$$

For kinetic energy of link OC point O is a pole, so:

$$T_{OC} = \frac{1}{2}\left(m_k \cdot (\dot{x}^2 + \dot{y}^2) - 2 \cdot K_r \cdot \dot{\psi} \cdot (\dot{x} \cdot cos(\psi) + \dot{y} \cdot sin(\psi)) + J \cdot \dot{\psi}^2\right) \tag{4.6}$$

Where $K_r = m_k \cdot r$;

m_k – Mass OC;

r – distance from O to OC mass center;

J – inertia moment OC relative point O;

In finding the kinetic energy for the body OC and hips OB and OD as a pole will take the point O. Similarly proceed for parts of BA and DE, as choosing as the pole point B and D. The process of withdrawal of these equations is also described in the works [40-41].

For kinetic energy of link OB point O is a pole, so:

$$T_{OB} = \frac{1}{2}\left(m_a \cdot (\dot{x}^2 + \dot{y}^2) + 2 \cdot m_a \cdot a \cdot \dot{\alpha_1} \cdot (\dot{x} \cdot cos(\alpha_1) + \dot{y} \cdot sin(\alpha_1)) + J_a^0 \cdot \dot{\alpha_1}^2\right) \tag{4.7}$$

where m_a – mass OB;

a – distance from O to OB mass centre;

J_a^0 – inertia moment OB relative point O;

For kinetic energy of link BA point B is a pole, so:

$$T_{BA} = \frac{1}{2}\left(m_b \cdot \left(\dot{x}^2 + \dot{y}^2 + 2 \cdot \dot{\alpha_1} \cdot L_a \cdot (\dot{x} \cdot cos(\alpha_1) + \dot{y} \cdot sin(\alpha_1)) + L_a^2 \cdot \dot{\alpha_1}^2\right) + 2 \cdot K_b \cdot \dot{\beta_1} \cdot (\dot{x} \cdot cos(\beta_1) + \dot{y} \cdot sin(\beta_1)) + J_b \cdot \dot{\beta_1}^2\right) \tag{4.8}$$

where $K_b = m_b \cdot b$;

m_b – mass BA;

b – distance from B to BA mass center;

L_a – length of OB;;

J_b – inertia moment BA relative point B;

T_{OD} and T_{DE} we can get from T_{OB} and T_{BA} by changing indexes from 1 to 2

$$T = T_{OC} + T_{OB} + T_{BA} + T_{OD} + T_{DE} = \frac{1}{2} \cdot M \cdot (\dot{x}^2 + \dot{y}^2) + \frac{1}{2} \cdot J \cdot \dot{\psi}^2 - K_r \cdot \dot{\psi} \cdot (\dot{x} \cdot cos(\psi) + \dot{y} \cdot sin(\psi)) + \sum_{i=1}^{2}[\frac{1}{2} \cdot J_a \cdot \dot{\alpha_i}^2 + \frac{1}{2} \cdot J_b \cdot \dot{\beta_i}^2 + K_a \cdot \dot{\alpha_i} \cdot \tag{4.9}$$

$\left(\dot{x} \cdot cos(\alpha_i) + \dot{y} \cdot sin(\alpha_i)\right) + K_b \cdot \dot{\beta_\iota} \cdot (\dot{x} \cdot cos(\beta_i) + \dot{y} \cdot sin(\beta_i)) + J_{ab} \cdot \dot{\alpha_\iota} \cdot \dot{\beta_\iota} \cdot cos(\alpha_i - \beta_i)\big]$

where:

$$M = m_k + 2 \cdot m_a + 2 \cdot m_b - \textit{total mass} \tag{4.10}$$

$$K_a = m_a \cdot a + m_b \cdot L_a \tag{4.11}$$

$$J_a = J_a^0 + m_b \cdot L_a^2 \tag{4.12}$$

$$J_{ab} = K_b \cdot L_a = m_b \cdot b \cdot L_a \tag{4.13}$$

For potential energy:

$$V = g \cdot \left[m_k \cdot (y + r \cdot cos(\psi)) + \sum_{i=1}^{2}\left(m_a \cdot (y - a \cdot cos(\alpha_i)) + m_b \cdot (y - L_a \cdot cos(\alpha_i) - b \cdot cos(\beta_i))\right)\right] = g \cdot [M \cdot y + K_r \cdot cos(\psi) - \sum_{i=1}^{2}(K_a \cdot cos(\alpha_i) + K_b \cdot cos(\beta_i))] \tag{4.14}$$

For equation (2.1) we find T and V, next we need to find Q_s, for this compare expression of elementary jobs:

$$\delta W = (R_{1x} + R_{2x}) \cdot \delta x + \left(R_{1y} + R_{2y}\right) \cdot \delta y - (q_1 + q_2) \cdot \delta\psi + \sum_{i=1}^{2}\left[(q_i - u_i) \cdot \delta\alpha_i + (u_i - P_i) \cdot \delta\beta_i + R_{1x} \cdot \delta(L_a \cdot sin(\alpha_i) + L_b \cdot sin(\beta_i)) - R_{1y} \cdot \delta(L_a \cdot cos(\alpha_i) + L_b \cdot cos(\beta_i))\right] = \sum_{i=1}^{2}\left[R_{ix} \cdot \delta x + R_{iy} \cdot \delta y - q_i \cdot \delta\psi + \left(q_i - u_i + R_{1x} \cdot L_a \cdot cos(\alpha_i) + R_{1y} \cdot L_a \cdot sin(\alpha_i)\right) \cdot \delta\alpha_i + \left(u_i - P_i + R_{1x} \cdot L_b \cdot cos(\beta_i) + R_{1y} \cdot L_b \cdot sin(\beta_i)\right) \cdot \delta\beta_i\right] \tag{4.15}$$

From (2.15):

$$Q_x = R_{1x} + R_{2x} \tag{4.16}$$

$$Q_y = R_{1y} + R_{2y} \tag{4.17}$$

$$Q_\psi = -q_1 - q_2 \tag{4.18}$$

$$Q_{\alpha_1} = q_1 - u_1 + R_{1x} \cdot L_a \cdot cos(\alpha_1) + R_{1y} \cdot L_a \cdot sin(\alpha_1) \tag{4.19}$$

$$Q_{\alpha_2} = q_2 - u_2 + R_{1x} \cdot L_a \cdot cos(\alpha_2) + R_{1y} \cdot L_a \cdot sin(\alpha_2) \tag{4.20}$$

$$Q_{\beta_1} = u_1 - P_1 + R_{1x} \cdot L_b \cdot cos(\beta_1) + R_{1y} \cdot L_b \cdot sin(\beta_1) \quad (4.21)$$

$$Q_{\beta_2} = u_2 - P_2 + R_{1x} \cdot L_b \cdot cos(\beta_2) + R_{1y} \cdot L_b \cdot sin(\beta_2) \quad (4.22)$$

4.3. Derivatives

This section identifies the first and second derivatives of the variables describing the system state.

Quotients derivative $\frac{\partial L}{\partial z}$:

$$\frac{\partial L}{\partial x} = \frac{\partial (T - V)}{\partial x} = 0 \quad (4.23)$$

$$\frac{\partial L}{\partial y} = \frac{\partial (T - V)}{\partial y} = -g \cdot M \quad (4.24)$$

$$\frac{\partial L}{\partial \psi} = \frac{\partial (T-V)}{\partial \psi} = K_r \cdot \left(\dot{x} \cdot \dot{\psi} \cdot sin(\psi) - \dot{y} \cdot \dot{\psi} \cdot cos(\psi) - g \cdot sin(\psi)\right) \quad (4.25)$$

$$\frac{\partial L}{\partial \alpha_i} = \frac{\partial (T-V)}{\partial \alpha_i} = K_a \cdot (\dot{\alpha_\iota} \cdot \dot{x} \cdot sin(\alpha_i) - \dot{\alpha_\iota} \cdot \dot{y} \cdot cos(\alpha_i) + g \cdot sin(\alpha_i)) - J_{ab} \cdot \dot{\alpha_\iota} \cdot \dot{\beta_\iota} \cdot sin(\alpha_i - \beta_i) \quad (4.26)$$

$$\frac{\partial L}{\partial \beta_i} = \frac{\partial (T-V)}{\partial \beta_i} = K_b \cdot \left(\dot{\beta_\iota} \cdot \dot{x} \cdot sin(\beta_i) - \dot{\beta_\iota} \cdot \dot{y} \cdot cos(\beta_i) + g \cdot sin(\beta_i)\right) - J_{ab} \cdot \dot{\alpha_\iota} \cdot \dot{\beta_\iota} \cdot sin(\alpha_i - \beta_i)\,; \quad (4.27)$$

Quotients derivative $\frac{\partial L}{\partial \dot{z}}$:

$$\frac{\partial L}{\partial \dot{x}} = M \cdot \dot{x} - K_r \cdot \dot{\psi} \cdot cos(\psi) + K_a \cdot \dot{\alpha}_i \cdot cos(\alpha_i) + K_b \cdot \dot{\beta}_i \cdot cos(\beta_i) \quad (4.28)$$

$$\frac{\partial L}{\partial \dot{y}} = M \cdot \dot{y} - K_r \cdot \dot{\psi} \cdot sin(\psi) + K_a \cdot \dot{\alpha}_i \cdot sin(\alpha_i) + K_b \cdot \dot{\beta}_i \cdot sin(\beta_i) \quad (4.29)$$

$$\frac{\partial L}{\partial \dot{\psi}} = J \cdot \dot{\psi} - K_r \cdot (\dot{x} \cdot cos(\psi) + \dot{y} \cdot sin(\psi)) \quad (4.30)$$

$$\frac{\partial L}{\partial \dot{\alpha}_i} = J_a \cdot \dot{\alpha}_i + K_a \cdot (\dot{x} \cdot cos(\alpha_i) + \dot{y} \cdot sin(\alpha_i)) + J_{ab} \cdot \dot{\beta}_i \cdot cos(\alpha_i - \beta_i) \quad (4.31)$$

$$\frac{\partial L}{\partial \dot{\beta}_i}=J_b\cdot\dot{\beta}_i+K_b\cdot\left(\dot{x}\cdot cos\left(\beta_i\right)+\dot{y}\cdot sin\left(\beta_i\right)\right)+J_{ab}\cdot\dot{\alpha}_i\cdot cos\left(\alpha_i\text{-}\beta_i\right) \tag{4.32}$$

Derivatives: $\frac{\mathrm{d}}{\mathrm{dt}}\cdot\frac{\partial \mathrm{L}}{\partial \dot{\mathrm{z}}}$:

$$\frac{d}{dt}\cdot\frac{\partial L}{\partial \dot{x}}=M\cdot\ddot{x}-K_r\cdot\ddot{\psi}\cdot cos(\psi)+K_r\cdot\dot{\psi}^2\cdot sin(\psi)+K_a\cdot\ddot{\alpha_\iota}\cdot cos(\alpha_i)-K_a\cdot\dot{\alpha_\iota}^2\cdot sin(\alpha_i)+K_b\cdot\ddot{\beta_\iota}\cdot cos(\beta_i)-K_b\cdot\dot{\beta_\iota}^2\cdot sin(\beta_i) \tag{4.33}$$

$$\frac{d}{dt}\cdot\frac{\partial L}{\partial \dot{y}}=M\cdot\ddot{y}-K_r\cdot\ddot{\psi}\cdot sin(\psi)-K_r\cdot\dot{\psi}^2\cdot cos(\psi)+K_a\cdot\ddot{\alpha_\iota}\cdot sin(\alpha_i)+K_a\cdot\dot{\alpha_\iota}^2\cdot cos(\alpha_i)+K_b\cdot\ddot{\beta_\iota}\cdot sin(\beta_i)+K_b\cdot\dot{\beta_\iota}^2\cdot cos(\beta_i) \tag{4.34}$$

$$\frac{d}{dt}\cdot\frac{\partial L}{\partial \dot{\psi}}=J\cdot\ddot{\psi}-K_r\cdot\left(\ddot{x}\cdot cos(\psi)+\ddot{y}\cdot sin(\psi)-\dot{x}\cdot\dot{\psi}\cdot sin(\psi)+\dot{y}\cdot\dot{\psi}\cdot cos(\psi)\right) \tag{4.35}$$

$$\frac{d}{dt}\cdot\frac{\partial L}{\partial \dot{\alpha_\iota}}=J_a\cdot\ddot{\alpha_\iota}+K_a\cdot(\ddot{x}\cdot cos(\alpha_i)+\ddot{y}\cdot sin(\alpha_i)+\dot{x}\cdot\dot{\alpha_\iota}\cdot sin(\alpha_i)-\dot{y}\cdot\dot{\alpha_\iota}\cdot cos(\alpha_i))+J_{ab}\cdot\ddot{\beta_\iota}\cdot cos(\alpha_i-\beta_i)-J_{ab}\cdot\dot{\beta_\iota}\cdot(\alpha_i-\beta_i)\cdot sin(\alpha_i-\beta_i) \tag{4.36}$$

$$\frac{d}{dt}\cdot\frac{\partial L}{\partial \dot{\beta_\iota}}=J_b\cdot\ddot{\beta_\iota}+K_b\cdot(\ddot{x}\cdot cos(\beta_i)+\ddot{y}\cdot sin(\beta_i)+\dot{x}\cdot\beta_i\cdot sin(\beta_i)-\dot{y}\cdot\beta_i\cdot cos(\beta_i))+J_{ab}\cdot\ddot{\alpha_\iota}\cdot cos(\alpha_i-\beta_i)-J_{ab}\cdot\alpha_\iota\cdot(\dot{\alpha_\iota}-\beta_\iota)\cdot sin(\alpha_i-\beta_i) \tag{4.37}$$

4.4. Dynamic equations for 5–link mechanism

And finally full Lagrange equations for 5–link mechanism:

$$M\cdot\ddot{x}-K_r\cdot\ddot{\psi}\cdot cos(\psi)+K_r\cdot\dot{\psi}^2\cdot sin(\psi)+K_a\cdot\ddot{\alpha_\iota}\cdot cos(\alpha_i)-K_a\cdot\dot{\alpha_\iota}^2\cdot sin(\alpha_i)+K_b\cdot\ddot{\beta_\iota}\cdot cos(\beta_i)-K_b\cdot\dot{\beta_\iota}^2\cdot sin(\beta_i)=R_{1x}+R_{2x},(i=1,2) \tag{4.38}$$

$$M\cdot\ddot{y}-K_r\cdot\ddot{\psi}\cdot sin(\psi)-K_r\cdot\dot{\psi}^2\cdot cos(\psi)+K_a\cdot\ddot{\alpha_\iota}\cdot sin(\alpha_i)+K_a\cdot\dot{\alpha_\iota}^2\cdot cos(\alpha_i)+K_b\cdot\ddot{\beta_\iota}\cdot sin(\beta_i)+K_b\cdot\dot{\beta_\iota}^2\cdot cos(\beta_i)=R_{1y}+R_{2y}-M\cdot g,(i=1,2) \tag{4.39}$$

$$-K_r\cdot\ddot{x}\cdot cos(\psi)-K_r\cdot\ddot{y}\cdot sin(\psi)+J\cdot\ddot{\psi}-K_r\cdot g\cdot sin(\psi)=-q_1-q_2,(i=1,2) \tag{4.40}$$

$$K_a\cdot\ddot{x}\cdot cos(\alpha_i)+K_a\ddot{\cdot} y\cdot sin(\alpha_i)+J_a\cdot\ddot{\alpha_\iota}+J_{ab}\cdot\ddot{\beta_\iota}\cdot cos(\alpha_i-\beta_i)+ \tag{4.41}$$

$$J_{ab} \cdot \dot{\beta_i}^2 \cdot sin(\alpha_i - \beta_i) + K_a \cdot g \cdot sin(\alpha_i) = q_i - u_i + R_{1x} \cdot L_a \cdot cos(\alpha_i) + R_{1y} \cdot L_a \cdot sin(\alpha_i), \ (i = 1,2);$$

$$K_b \cdot \ddot{x} \cdot cos(\beta_i) + K_b \cdot \ddot{y} \cdot sin(\beta_i) + J_b \cdot \ddot{\beta_i} + J_{ab} \cdot \ddot{\alpha_i} \cdot cos(\alpha_i - \beta_i) - J_{ab} \cdot \dot{\alpha_i}^2 \cdot sin(\alpha_i - \beta_i) + K_b \cdot g \cdot sin(\beta_i) = u_i - P_i + R_{1x} \cdot L_b \cdot cos(\beta_i) + R_{1y} \cdot L_b \cdot sin(\beta_i), (i = 1,2) \quad (4.42)$$

Equations (4.38) - (4.42) are also obtained in [42, 43].

These equations describe dynamic of 5-link model, but our model has limited movement, point A or E must be fixed on the surface:

If point A fixed, we have kinematic equations for x and y:

$$x = x_A - L_a \cdot sin(\alpha_1) - L_b \cdot sin(\beta_1) \quad (4.43)$$

$$y = y_A + L_a \cdot cos(\alpha_1) + L_b \cdot cos(\beta_1) \quad (4.44)$$

$$\dot{x} = -L_a \cdot \dot{\alpha_1} \cdot cos(\alpha_1) - L_b \cdot \dot{\beta_1} \cdot cos(\beta_1) \quad (4.45)$$

$$\dot{y} = -L_a \cdot \dot{\alpha_1} \cdot sin(\alpha_1) - L_b \cdot \dot{\beta_1} \cdot sin(\beta_1) \quad (4.46)$$

New equations for T, V and δW (4.9, 4.14, 2.15 with 4.43-4.46):

$$T = \frac{1}{2} \cdot J \cdot \dot{\psi}^2 + \frac{1}{2} \cdot M \cdot \left(J_a - 2 \cdot L_a \cdot K_a + {L_a}^2 \cdot M\right) \cdot \dot{\alpha_1}^2 + \frac{1}{2} \cdot J_a \cdot \dot{\alpha_2}^2 + \frac{1}{2} \cdot M \cdot \left(J_b - 2 \cdot L_b \cdot K_b + {L_b}^2 \cdot M\right) \cdot \dot{\beta_1}^2 + \frac{1}{2} \cdot J_a \cdot \dot{\beta_2}^2 + L_a \cdot K_r \cdot cos(\psi - \alpha_1) \cdot \dot{\psi} \cdot \dot{\alpha}_1 + L_b \cdot K_r \cdot cos(\psi - \beta_1) \cdot \dot{\psi} \cdot \dot{\beta}_1 - L_a \cdot K_a \cdot cos(\alpha_1 - \alpha_2) \cdot \dot{\alpha}_1 \cdot \dot{\alpha}_2 + (J_{ab} - L_a \cdot K_b - L_b \cdot K_a + L_a \cdot L_b \cdot M) \cdot cos(\alpha_1 - \beta_1) \cdot \dot{\alpha}_1 \cdot \dot{\beta}_1 - L_a \cdot K_b \cdot cos(\alpha_1 - \beta_2) \cdot \dot{\alpha}_1 \cdot \dot{\beta}_2 - L_b \cdot K_a \cdot cos(\alpha_2 - \beta_1) \cdot \dot{\alpha}_2 \cdot \dot{\beta}_1 + L_b \cdot K_b \cdot cos(\beta_1 - \beta_2) \cdot \dot{\beta}_1 \cdot \dot{\beta}_2 \quad (4.47)$$

$$V = g \cdot [M \cdot y_A + K_r \cdot cos(\psi) + (L_a \cdot M - K_a) \cdot cos(\alpha_1) - K_a \cdot cos(\alpha_2) + (L_b \cdot M - K_b) \cdot cos(\beta_1) - K_b \cdot cos(\beta_2)] \quad (4.48)$$

$$\delta W = -(q_1 + q_2) \cdot \delta\psi + \left(q_1 - u_1 - R_{2x} \cdot L_a \cdot cos(\alpha_1) - R_{2y} \cdot L_a \cdot sin(\alpha_1)\right) \cdot \delta\alpha_1 + \left(q_2 - u_2 - R_{2x} \cdot L_a \cdot cos(\alpha_2) - R_{2y} \cdot L_a \cdot sin(\alpha_2)\right) \cdot \delta\alpha_2 + \left(u_1 - P_1 - R_{2x} \cdot L_b \cdot cos(\beta_1) - R_{2y} \cdot L_b \cdot sin(\beta_1)\right) \cdot \delta\beta_1 + \left(u_2 - P_2 - R_{2x} \cdot L_b \cdot cos(\beta_2) - R_{2y} \cdot L_b \cdot sin(\beta_2)\right) \cdot \delta\beta_2 \quad (4.49)$$

Equations in form (1) will be too big and difficult to work with them. In matrix form, they look like:

$$B_l \cdot \ddot{z_\iota} + g \cdot A \cdot sin(z_i) + D(z) \cdot \dot{z_\iota}^2 = C(z) \cdot \omega \tag{4.50}$$

Where $z_i = \begin{bmatrix} \varphi \\ \alpha_1 \\ \alpha_2 \\ \beta_1 \\ \beta_2 \end{bmatrix}$, $\sin(z_i) = \begin{bmatrix} \sin\varphi \\ \sin\alpha_1 \\ \sin\alpha_2 \\ \sin\beta_1 \\ \sin\beta_2 \end{bmatrix}$, $\dot{z_\iota}^2 = \begin{bmatrix} \dot{\varphi}^2 \\ \dot{\alpha_1}^2 \\ \dot{\alpha_2}^2 \\ \dot{\beta_1}^2 \\ \dot{\beta_2}^2 \end{bmatrix}$, $\omega = \begin{bmatrix} u_1 \\ u_2 \\ q_1 \\ q_2 \\ P_1 \\ P_2 \\ R_{2x} \\ R_{2y} \end{bmatrix}$.

Matrix B(z) is a symmetric and positive definite matrix. B(z) can be named as kinetic energy matrix, because:

$$T = T(z, \dot{z}) = \frac{1}{2} \cdot \dot{z} \cdot B(z) \cdot \dot{z} \tag{4.51}$$

$$B(z)=\begin{bmatrix} J & L_a \cdot K_r \cdot \cos(\varphi-\alpha_1) & 0 & L_b \cdot K_r \cdot \cos(\varphi-\beta_1) & 0 \\ L_a \cdot K_r \cdot \cos(\varphi-\alpha_1) & J_a-2 \cdot L_a \cdot K_a+L_a^2 \cdot M & -L_a \cdot K_a \cdot \cos(\alpha_1-\alpha_2) & (J_{ab}-L_a \cdot K_b-L_b \cdot K_a+L_a \cdot L_b \cdot M) \cdot \cos(\alpha_1-\beta_1) & -L_a \cdot K_b \cdot \cos(\alpha_1-\beta_2) \\ 0 & -L_a \cdot K_a \cdot \cos(\alpha_1-\alpha_2) & J_a & -L_b \cdot K_a \cdot \cos(\alpha_2-\beta_1) & J_{ab} \cdot \cos(\alpha_2-\beta_2) \\ L_b \cdot K_r \cdot \cos(\varphi-\beta_1) & (J_{ab}-L_a \cdot K_b-L_b \cdot K_a+L_a \cdot L_b \cdot M) \cdot \cos(\alpha_1-\beta_1) & -L_b \cdot K_a \cdot \cos(\alpha_2-\beta_1) & J_b-2 \cdot L_b \cdot K_b+L_b^2 \cdot M & -L_b \cdot K_b \cdot \cos(\beta_1-\beta_2) \\ 0 & -L_a \cdot K_b \cdot \cos(\alpha_1-\beta_2) & J_{ab} \cdot \cos(\alpha_2-\beta_2) & -L_b \cdot K_b \cdot \cos(\beta_1-\beta_2) & J_b \end{bmatrix}$$

Matrix A is a diagonal matrix, named as matrix of potential energy, because:

$$V = V(z) = g \cdot (M \cdot y_A - \sum_{i=1}^{5} a_{ii} \cdot cos z_i) \tag{4.52}$$

Where a_{ii} are diagonal elements of A:

$$A = \begin{bmatrix} -K_r & 0 & 0 & 0 & 0 \\ 0 & K_a - L_a \cdot M & 0 & 0 & 0 \\ 0 & 0 & K_a & 0 & 0 \\ 0 & 0 & 0 & K_b - L_b \cdot M & 0 \\ 0 & 0 & 0 & 0 & K_b \end{bmatrix}$$

Matrix D(z) is skew-symmetric matrix ($d_{ij}(z) = -d_{ji}(z)$. Elements of matrix D(z) is Christoffel symbols of the first kind for matrix B(z).

$$D(z)=\begin{bmatrix} 0 & L_a \cdot K_r \cdot sin(\varphi-\alpha_1) & 0 & L_b \cdot K_r \cdot sin(\varphi-\beta_1) & 0 \\ -L_a \cdot K_r \cdot sin(\varphi-\alpha_1) & 0 & -L_a \cdot K_a \cdot sin(\alpha_1-\alpha_2) & (J_{ab}-L_a \cdot K_b-L_b \cdot K_a+L_a \cdot L_b \cdot M) \cdot sin(\alpha_1-\beta_1) & -L_a \cdot K_b \cdot sin(\alpha_1-\beta_2) \\ 0 & L_a \cdot K_a \cdot sin(\alpha_1-\alpha_2) & 0 & -L_b \cdot K_a \cdot sin(\alpha_2-\beta_1) & J_{ab} \cdot sin(\alpha_2-\beta_2) \\ -L_b \cdot K_r \cdot sin(\varphi-\beta_1) & -(J_{ab}-L_a \cdot K_b-L_b \cdot K_a+L_a \cdot L_b \cdot M) \cdot sin(\alpha_1-\beta_1) & L_b \cdot K_a \cdot sin(\alpha_2-\beta_1) & 0 & -L_b \cdot K_b \cdot sin(\beta_1-\beta_2) \\ 0 & L_a \cdot K_b \cdot sin(\alpha_1-\beta_2) & -J_{ab} \cdot sin(\alpha_2-\beta_2) & L_b \cdot K_b \cdot sin(\beta_1-\beta_2) & 0 \end{bmatrix}$$

$$C(z) = \begin{bmatrix} 0 & 0 & -1 & -1 & 0 & 0 & 0 & 0 \\ -1 & 0 & 1 & 0 & 0 & 0 & -L_a \cdot \cos\alpha_1 & -L_a \cdot \sin\alpha_1 \\ 0 & -1 & 0 & 1 & 0 & 0 & L_a \cdot \cos\alpha_2 & L_a \cdot \sin\alpha_2 \\ 1 & 0 & 0 & 0 & -1 & 0 & -L_b \cdot \cos\beta_1 & -L_b \cdot \sin\beta_1 \\ 0 & 1 & 0 & 0 & 0 & -1 & L_b \cdot \cos\beta_2 & L_b \cdot \sin\beta_2 \end{bmatrix}$$

4.5. Linearization

Next we considering singly movement phase (when $\dot{y_A} = \dot{x_A} = 0;\ \dot{y_E} \neq 0;\ \dot{x_E} \neq 0;$)

If in movement z_i and $\dot{z}_i$ are small we can linearize movement equations around point $z_i = 0,\ \dot{z}_i = 0$, $(i = 1, \dots, 5)$. These equations describe the state of equilibrium when $\omega(t) = 0$. This state corresponds to the vertical arrangement of all parts of the mechanism (5-link stands on one leg). Note that reporting a five-link mechanism is pivotally mounted end of the supporting leg can have $2^5 = 32$ the equilibrium position. This follows from the fact that the mechanism of equilibrium each of the links can be a vertikalyo angle equal to zero or $180°$.

After that movement equations take the form:

$$\ddot{z}_l \cdot B_l + g \cdot A \cdot z_i = C_l \cdot \omega \qquad (4.53)$$

And from matrix B(z) and C(z) we can get B_l and C_l:

$$B_l = \begin{bmatrix} J & L_a \cdot K_r & 0 & L_b \cdot K_r & 0 \\ L_a \cdot K_r & J_a - 2 \cdot L_a \cdot K_a + L_a^2 \cdot M & -L_a \cdot K_a & (J_{ab} - L_a \cdot K_b - L_b \cdot K_a + L_a \cdot L_b \cdot M) & -L_a \cdot K_b \\ 0 & -L_a \cdot K_a & J_a & -L_b \cdot K_a & J_{ab} \\ L_b \cdot K_r & (J_{ab} - L_a \cdot K_b - L_b \cdot K_a + L_a \cdot L_b \cdot M) & -L_b \cdot K_a & J_b - 2 \cdot L_b \cdot K_b + L_b^2 \cdot M & -L_b \cdot K_b \\ 0 & -L_a \cdot K_b & J_{ab} & -L_b \cdot K_b & J_b \end{bmatrix}$$

$$C_l = \begin{bmatrix} 0 & 0 & -1 & -1 & 0 & 0 & 0 & 0 \\ -1 & 0 & 1 & 0 & 0 & 0 & -L_a & -L_a \cdot \alpha_1 \\ 0 & -1 & 0 & 1 & 0 & 0 & L_a & L_a \cdot \alpha_2 \\ 1 & 0 & 0 & 0 & -1 & 0 & -L_b & -L_b \cdot \beta_1 \\ 0 & 1 & 0 & 0 & 0 & -1 & L_b & L_b \cdot \beta_2 \end{bmatrix}$$

Note that the matrix B under the sign of the cosine of the included angle difference. While the absolute value of each of the corners may be small, for example, may not exceed $30°$, angle difference may be large. The validity of such a linearization depends on the stride length. For large steps linearization is not applicable.

With $\omega(t) = 0$ we can get equations of linearized ballistic motion for 5-link model:

$$B_l \cdot \ddot{z}_l + g \cdot A \cdot z_i = 0 \quad (4.54)$$

And

$$\ddot{z}_l + g \cdot {B_l}^{-1} \cdot A \cdot z_i = 0 \quad (4.55)$$

4.6. Solving

A boundary value problem for the system (4.54) or (4.55) is formulated as follows: find a solution $z(t) = 0$ of the system (4.54), which at the time $t = 0$ and $t = T$ passes through specified in the configuration space of the point $z(0)$ and $z(T)$. Let us find a solution to this boundary value problem.

After that, as soon as (4.55) is a conservative linear steady-state system, we can use linear non-singular transformation with constant coefficients:

$$z = Rx \quad (4.56)$$

In normal coordinates eqn. (4.55) after transformation (4.56) have form [43-44]:

$$\ddot{x} + \Omega \cdot x = 0 \quad (4.57)$$

where Ω is diagonal 5x5 matrix:

$$\Omega = \begin{bmatrix} \lambda_1 & 0 & 0 & 0 & 0 \\ 0 & \lambda_2 & 0 & 0 & 0 \\ 0 & 0 & \lambda_3 & 0 & 0 \\ 0 & 0 & 0 & \lambda_4 & 0 \\ 0 & 0 & 0 & 0 & \lambda_5 \end{bmatrix},$$

where λ_i are roots of characteristic equation of Ω:

$$det(B_l \cdot \lambda + g \cdot A) = 0 \quad (4.58)$$

Some methods of construction of the transformation (4.56) are presented in [43-44]. Note that the matrix Ω and R in Matlab software package can be calculated using the function "$eig(inv(\boldsymbol{B}) \cdot g \cdot A)$".

The matrix R is known [42-43] resulting in a symmetric positive definite matrix B_l to the unit and the symmetric matrix A – to the diagonal. So for matrix R we have equations:

$$R^T \cdot B_l \cdot R = E \quad (4.59)$$

$$R^T \cdot g \cdot A \cdot R = \Omega \quad (4.60)$$

From the law of inertia of quadratic forms we have: among the numbers λ_i as positive (negative) as positive (negative) eigenvalues of a matrix A.
So in matrix A we have 3 negative and 2 positive elements and denote:

$$\lambda_i = \omega_i^2 > 0 \text{ for } 2\ \lambda_i \text{ and } \lambda_i = -\omega_i^2 < 0 \text{ for } 3\ \lambda_i$$

It means we have 2 equations:

$$\ddot{x}_i + \omega_i^2 \cdot x_i = 0 \; for \; i = 3{,}5 \tag{4.61}$$

$$\ddot{x}_i - \omega_i^2 \cdot x_i = 0 \; for \; i = 1{,}2{,}4 \tag{4.62}$$

Vectors of the initial and final conditions:

$$x(0) = R^{-1} \cdot z(0), x(T) = R^{-1} \cdot z(T) \tag{4.63}$$

And decision of this equations (9):

$$x_i(t) = \frac{\dot{x}_i(0)}{\omega_i} \cdot sin(\omega_i t) + x_i(0) \cdot cos(\omega_i t) \tag{4.64}$$

$$\dot{x}_i(0) = \omega_i \cdot \frac{x_i(T) - x_i(0) \cdot cos(\omega_i T)}{sin(\omega_i t)} \tag{4.65}$$

After substitution (13) in (12) we have:

$$x_i(t) = \frac{x_i(T)\, sin(\omega_i T) + x_i(0) \cdot sin\big(\omega_i (T - t)\big)}{sin(\omega_i t)} \quad i = 3{,}5 \tag{4.66}$$

For (10) we have analogical decision:

$$x_i(t) = \frac{x_i(T)\, sh(\omega_i T) + x_i(0) \cdot sh(\omega_i (T - t))}{sh(\omega_i t)} \quad i = 1{,}2{,}4 \tag{4.67}$$

Equations (4.66) (4.67) describe the solution of the boundary problem for the system (4.57). This solution is unique in all the boundary condition x (0) and x (T). Using the transformation (4.56), the original variables can be returned, and a solution of the boundary problem for a linear system (4.54) can be deduced. Thus, the transition to the normal coordinates allows us to write the solution of the boundary value problem for the system (4.54) with the help of equations (4.66), (4.67).

4.7. Mathematical model results

As a result, it developed a mathematical model of 5-link mechanism for the movement of which is described solely by the initial moment of inertia, the start and end positions, as well as anthropometric parameters. Fig. 2.4-2.7 is a comparison analysis of the trajectories and the experimental data obtained with Vicon motion capture system.

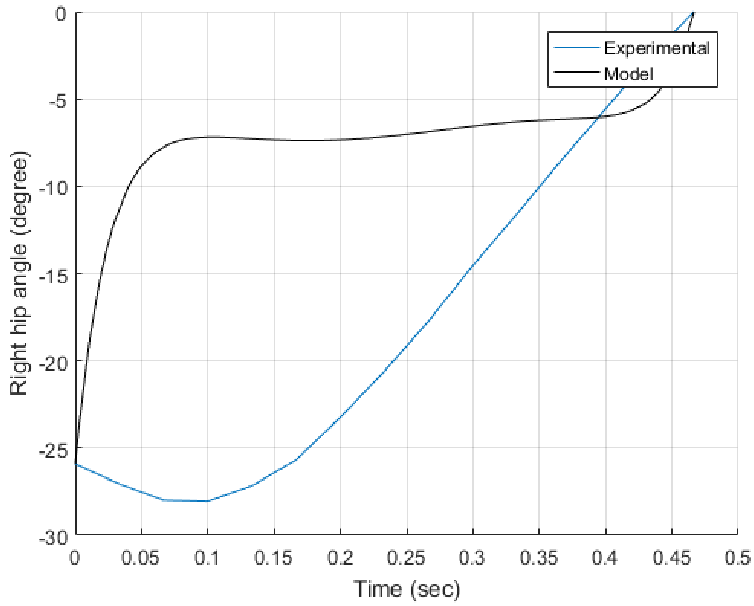

Figure 4.3: Right hip angles

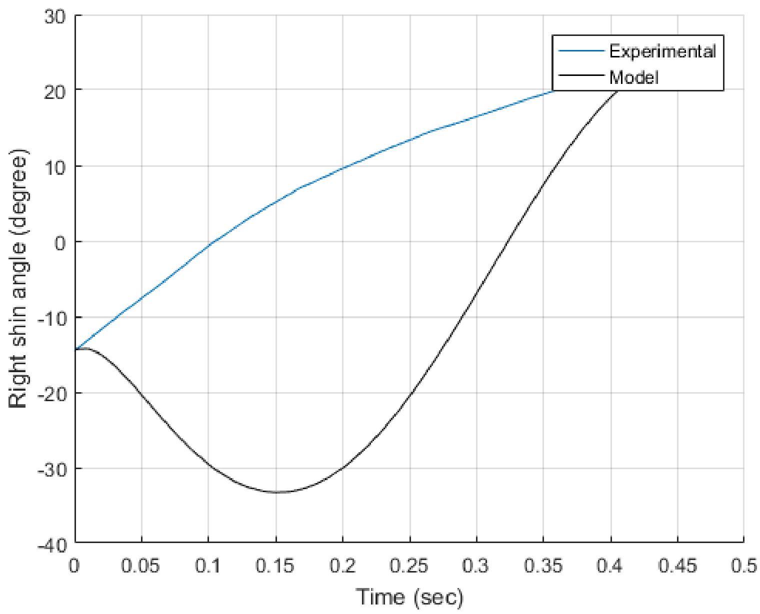

Figure 4.4: Right shin angles

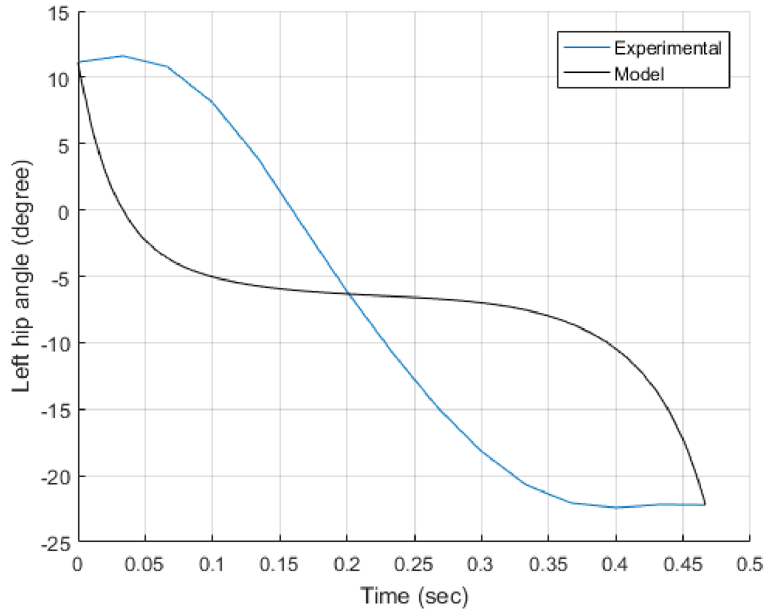

Figure 4.6: Left hip angles

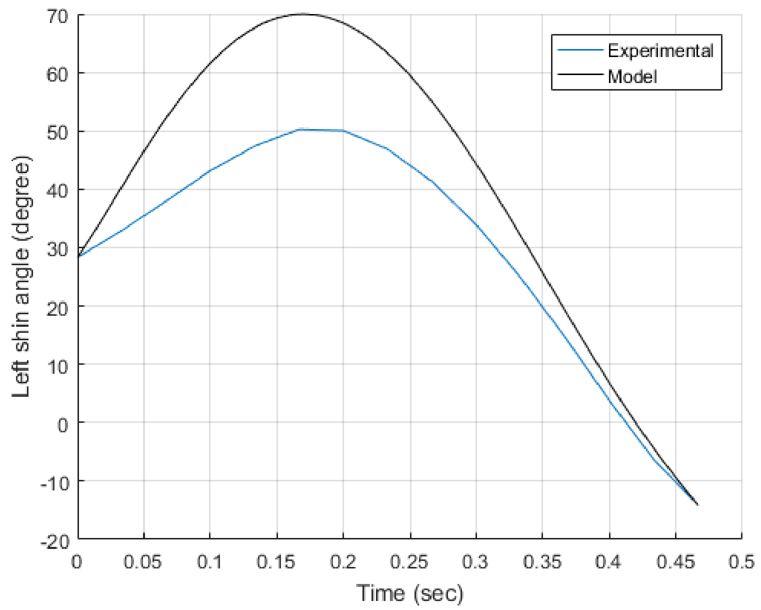

Figure 4.7: Left shin angles

As can be seen from Fig. 4.4-4.7, the linearized model of the system leads to the correct end results, as was originally defined, but the kinematics model and a man differ in almost everything. However, the dynamics of motion left (in this case, portable) shin coincides with the experimental data. But as limiting foot traffic were not included in mathematical formulas 4.66-4.77, the amplitude of the motion is more than the required by 20°. It is also worth noting that in [47], which is designed model with the MPC and PID controls, one of the biggest mistakes just in traffic carried by the left shin.

4.8. Conclusion

This chapter describes the output of a mathematical model, as well as the results of such a model and compared with experimental data. As a result, movement of the model was obtained idealized anthropomorphic mechanism, which is similar to human movement, but they are not. This mathematical hereinafter be used to describe the desired motion of the tibia tolerated because MPC will not raise the leg as high as this one does, and the mathematical model describes it more successfully.

5. DESIGN OF MPC

Introduced earlier algorithm to compute angles, allows to know only the approximate nature of the movement, as in most of the mathematical model does not take into account the maximum possible points, as well as the linearization of supposed impulse control, when the character of the movement is given only at the moment of pushing away, and then the system is coasting. For further operation of the system and calculate the necessary moments of MPC control model has been chosen, which the algorithm should be developed so that it functioned as the central nervous system. In the classical feedback control, the control inputs are regulated on the basis of past mistakes, but in this case you need to reverse - control based on predictions of output and control input regulation in advance of such a control system is the MPC. After you select the general type of control method, it is necessary to choose which one you want to use version of the MPC. This chapter describes how the parameters MPC, associated with the human gait and which branch MPC used were developed. Firstly, the basic principle described by MPC; Second, the critical aspects of the MPC are studied and related to human gait, and the justification for the control of nonlinear MPC endpoint explained.

5.1. General Concept of MPC

As mentioned earlier, all control based methods can be divided into two categories: management based on past mistakes and management based on the prediction. Most control methods fall into the first category, where the control input is generated based on the difference between the output signals and the target model. A block diagram of this type of control algorithm is shown in Fig. 3.1.

Control with PID controller is still the most common type of control algorithm in the industry. The reason is that it is simple, easy to adapt and configure.

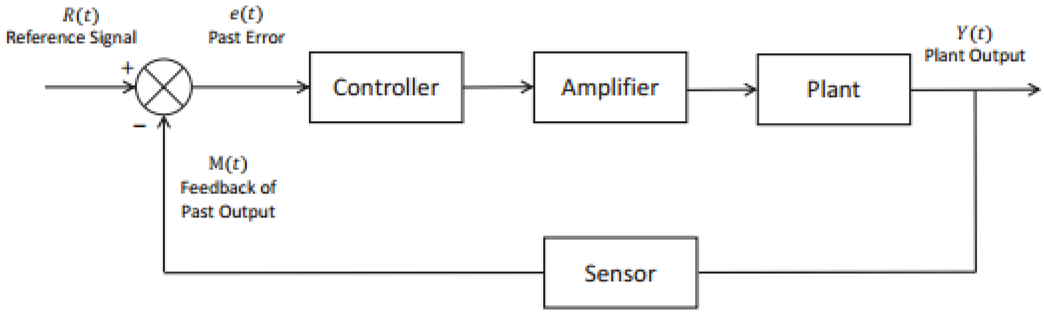

Figure 5.1: Past error control method

Model predictive control (MPC) is a promising method of process control, which is used in manufacturing, for example, mountain, chemical, and oil refineries. MPC uses models to predict the future behavior of the controlled variables. Based on the forecast, the controller calculates control actions by solving the optimization problem in real time. In this case, the controller tries to minimize the error between the predicted and actual value for the control horizon, i.e. implemented the first control action. The bases of the MPC controllers are dynamic process model, often linear empirical models obtained by system identification.

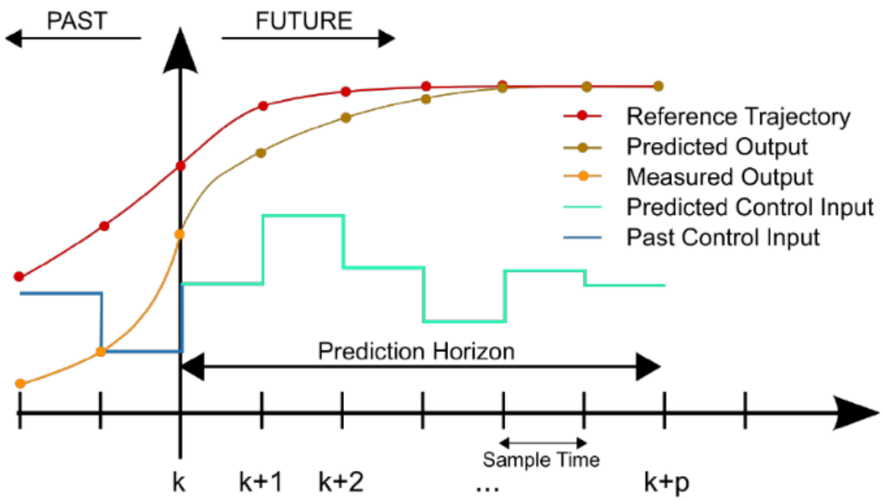

Figure 5.2: MPC system

All UPM algorithms have common elements, and for each item, you can choose various options, which gives grounds for the application of different algorithms. These elements are:

- *Forecasting model;*
- *Objective function;*
- *Control law.*

This prediction model is the most important part of MPC. Full project should include the necessary mechanisms for the optimal model, which should be complete enough to cover all the dynamic characteristics of the process and calculate predictions and simultaneously intuitive to conduct a theoretical analysis. Using a process model is determined by the need to calculate the predicted output at future points in time. The basic principle of operation is shown in fig. 3.2.

The following is an overview of the principles MPC customization in terms of theory and practice. We discuss the basic steps improve performance controllers. Setting parameters of controllers are discussed on the basis of the wording of the control law.

However, the central nervous system working principle is very different from the control on the basis of past mistakes, feedback should be used to predict the future position and the change of the control input must occur before the error itself. For example, a person sees an obstacle that will inevitably cause an error if continue driving in the same form. In this case, the system should, without waiting for failure (error), to change behavior to avoid mistakes at all. Thus, the central nervous system changes, the moments in the joints and the person passes or steps over an obstacle. If in this case, any control algorithm was used on the basis of an error, the system will first be faced with an obstacle, and then later tried to continue driving.

Just people presupposes, where he will be some time, though she walking and the decision to move to a certain other position, is the work of several different levels. Also, if we consider any movement of human joints in general, one first assumes, for any trajectory will move the joint, such as a kick on punching bag at a specific point, the CNS level, which is considered in this chapter, based on what, where and how should hit the foot calculates necessary points for such movement. This same strategy is to use movement of CNS and other body parts, such as arms in fig. 3.3 [45].

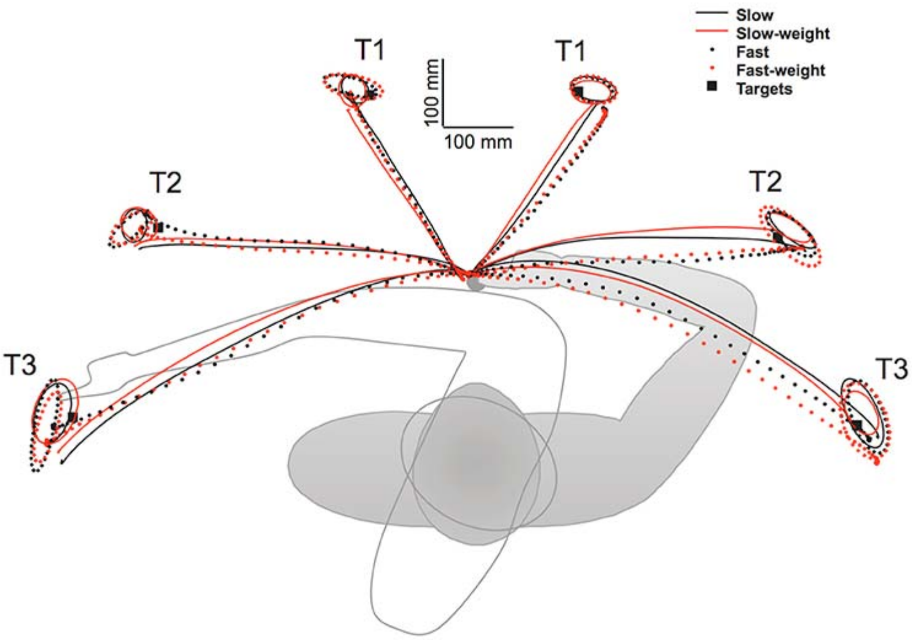

Figure 5.3: CNS Prediction

Some aspects of the MPC system determine how it will work in principle. Therefore, they should be described as a choice of various options MPCs which have a decisive role. To implement the MPC control, internal model is used to predict future performance installation based on the current state and future of plant control inputs. Internal model plays an important role in the control system. Developed internal model should be able to capture the dynamics of the plant to adequately predict future outputs, and at the same time, to be simple enough to be modeled.

5.2. The internal model of MPC

In the chemical engineering industry, where the MPC was originally designed, the most popular type of internal model is an empirical model, which is very easy to get, as it requires the measurement of the output signal only when the plant is driven by a step or pulse input. This type of model has been widely accepted in the industry, as it is very intuitive and can be used for highly nonlinear processes. Disadvantages of empirical models are a large number of parameters required and applicable only to the open-loop stable processes. In addition, the most important disadvantage of using an empirical model for this study is that it does not give any representation or of the dynamics of human gait and CNS principles.

Another possible type of internal MPC model is the model of the state space, which is widely used both in industry and research. SS model describes mathematical process to install in the time domain. The general expression of continuous-time state-space model is:

$$\dot{x} = A \cdot x + B \cdot u \tag{5.1}$$

$$y = C \cdot x + D \cdot u \tag{5.2}$$

Where the first equation is called the state equation and second equation is called the output equation. And $x(t)$ represents the states, $u(t)$ represents the inputs, $y(t)$ represents the outputs. For a model with Nx states, Ny outputs, and Nu inputs:

- *A is an Nx-by-Nx real- or complex-valued matrix.*
- *B is an Nx-by-Nu real- or complex-valued matrix.*
- *C is an Ny-by-Nx real- or complex-valued matrix.*
- *D is an Ny-by-Nu real- or complex-valued matrix.*

Even a very non-linear and multi-dimensional process can be represented by models of the state-space, which also has a well-developed stability and reliability criteria. More importantly, the state-space model provides insight into the dynamic process of installation. Therefore state-space approach will be used for constructing inner MPC model.

For the model of 5-mer mechanism, described in Chapter 3, by linearization were obtained matrix A, B, C, and D; wherein:

- *A is an 10x10 real matrix*
- *B is an 10x5 real matrix*
- *C is an 5x10 real matrix*
- *D is an zero matrix*
-

5.3. Objective function

After the internal model MPC is designed, the objective function must be set to determine the optimal future costs. The overall objective for the objective function, J, is that the predicted future output along the prediction horizon P should be as close as possible to the standard, while the control inputs used must be minimal. This philosophy may be expressed as [42]:

$$J(x(0), u) = \frac{1}{2} \sum_{k=N_0}^{N-1} [x(k)^T \cdot Q \cdot x(k) + u(k)^T \cdot R \cdot u(k)] + \frac{1}{2} x(N)^T \cdot Q_f \cdot x(N) \tag{5.3}$$

Where N_0 is normally the current time, which is normally 0, N is the final time step, Q is the weighting matrix for the predicted states along the prediction horizon, R is the weighting matrix for the control inputs, and Q_f is the weighting matrix for the final predicted states at the final time step.

There are three terms in the equation 3.3. The first term is associated with $x(k)$ is called the Stage cost, the second term is due to $u(k)$ is called the Control Input cost, and the last term is due to $x(N)$ is a Terminal Cost. By adjusting the relative ratio between the weight matrices Q, R, and Q_f, the relative importance of the three different value can be adjusted. This feature proves MPC powerful application for gait design model, and provides a significant advantage over the traditional PID control.

5.4. Constraints

Another advantage compared to conventional MPC PID control is that the MPC can explicitly include restrictions to the controller. Control inputs for each physical system have a number of limitations. In this thesis, for example, the maximum input torque generated from human joints such as ankles, knees and hips are limited. These constraints can be expressed as follow:

$$\min(u(k)) < u(k) < \max(u(k)) \tag{5.4}$$

By analogy with the constraints on control input, it is also desirable to impose restrictions on the state of the safety and feasibility of the plant. In human gait, for example, there are limitations on the range of motion for each of the joints. This can be expressed as follows:

$$\min(y(k)) < y(k) < \max(y(k)) \tag{5.5}$$

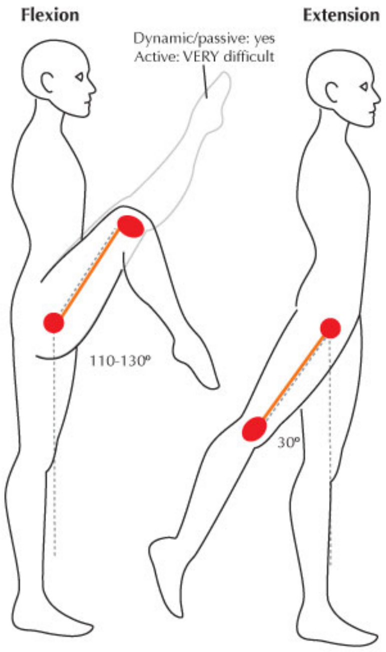

Figure 5.4: Human Constrains

Except the maximum and minimum values of inputs and outputs, you can set them to the maximum rate of change, which certainly allows you to personalize a controller under the human parameters. For example, we can limit the maximum and minimum points are created in the joints, then the parameters and dynamics of the MPC controller operation will be significantly different for people with different force. Likewise, you can assume human movement, whose work specific muscles broken or non-existent. Again with the help of these constraints can be defined different types of gaits, for example, specifically limited or defined rotation angles at special steps. Hip constraints of healthy human presented in fig. 5.4.

5.5. MPC strategy

Before creating the MPC control system must take into account the structure of the MPC. Decisions need to be made include whether to use linear or non-linear representation space of states for internal MPC models, the end point or continuous MPC control. These decisions directly affect the performance model of the human gait.

There are two possible types of models state-space, to describe the dynamic process of the target audience: a linear or non-linear model state-space. Each dynamic process is actually a non-linear process. Thus, the inherent advantage of a nonlinear model state-space is that it can describe the dynamic processes more accurately. However, for some simple engineering applications linear state-space model can describe the dynamic process is very good, because non-linear dynamics are subtle or out of range; such nonlinearities can be ignored without any apparent degradation of performance. For other situations, even though the dynamic process of installation can be substantially non-linear, the plant serves approximately one operating point; so the non-linear model state-space can be linearized around this operating point and converted into a linear model. In these cases, the linear model state-space, are preferred since they can be easily integrated and can be implemented in real time.

In this work for the internal model state-space are taken nonlinear model state-space. Since management must occur in real time, as well as in Chapter 4 was presented a linearized model from the results of which, it was concluded that for the modeling of human gait, clearly nonlinear model should be used. Ditto for linearization would require the use of steady-state operating point, which is not in the continuous human movement.

5.6. End-point or continuous MPC control

Epy target management MPC function has the general form:

$$J(x(0),u) = \frac{1}{2}\sum_{k=N_0}^{N-1}\left[x(k)^T \cdot Q \cdot x(k) + u(k)^T \cdot R \cdot u(k)\right] + \frac{1}{2}x(N)^T \cdot Q_f \cdot x(N) \tag{5.4}$$

Where Q is the weighting matrix for the predicted states along the prediction horizon, R is the weighting matrix for the control inputs, and Q_f is the weighting matrix for the final predicted states at the final time step. with x(k) is called the Stage cost, the second term is due to u(k) is called the Control Input cost, and the last term is due to x(N) is a Terminal Cost. If the weight matrix $Q_f = 0$, the objective function will look like this:

$$J(x(0),u) = \frac{1}{2}\sum_{k=N_0}^{N-1}[x(k)^T \cdot Q \cdot x(k) + u(k)^T \cdot R \cdot u(k)] \tag{5.5}$$

Thus, the terminal value is ignored, and the controller outputs focused on during the process. This management strategy is called continuous Control MPC. In contrast, if the weight matrix $Q = 0$, then the target function would be:

$$J(x(0),u) = \frac{1}{2}\sum_{k=N_0}^{N-1} u(k)^T \cdot R \cdot u(k) + \frac{1}{2}x(N)^T \cdot Q_f \cdot x(N) \tag{5.4}$$

In this case, the output signals are ignored during the process, and to bring the focus controller output links at the end of the process. This management strategy is called the End-Point MPC Control. MPC therefore can emphasize either the process or the final results.

For this model, it is assumed that should be used by End-Point MPC Control, to accurately achieve the critical points (target position).

5.7. Prediction horizon, control horizon

Another two important parameters must be defined for any MPC system. These parameters are the prediction horizon and control horizon. Prediction horizon determines how long the MPC will predict the state of the system, with the help of the substitution of possible future control inputs to the internal model MPC. Control horizon determines how many how many time steps will be optimized for the control inputs. Typically, larger values of prediction horizon and control horizon give greater precision controller, but require more calculations. Therefore it is necessary to determine the optimal values of horizons optimally working of the system. A visual representation of the prediction and control horizons is shown in the fig. 5.5.

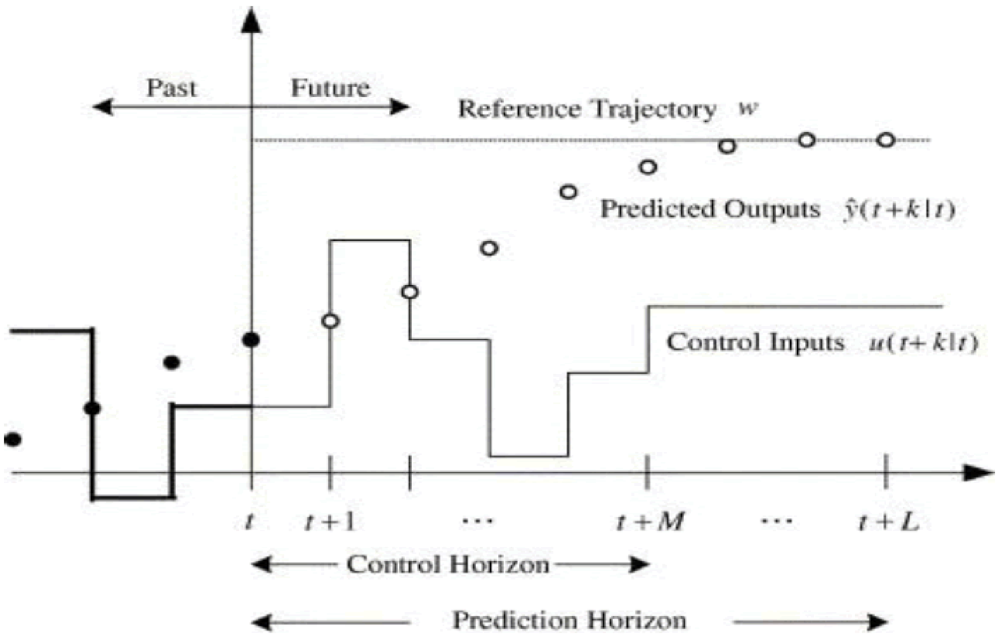

Figure 5.5: MPC horizons

Since end-point MPC is used for both Single Support and Double Support Phase simulation, the Prediction and Control Horizon are from the current time step to the end time step of the respective phases. Therefore the Prediction and Control Horizon are not constant and decrease as time progresses.

To give an example of how P (Prediction horizon) and C (Control Horizon) changes as time goes on, let $t = 1$ and the last time step $N = 50$, MPC controller predicts future states and optimizes future control inputs from the first time step until the final 50 time step; Therefore, $P = C = 49$. When a current flows during the next time step $t = 2$, MPC controller predicts a future state, and optimizes the control inputs of the second time step up to the last time step 50, making the $P = C = 48$. Thus forecast reduction Horizon Horizon and management, as time goes on.

5.8. Summary

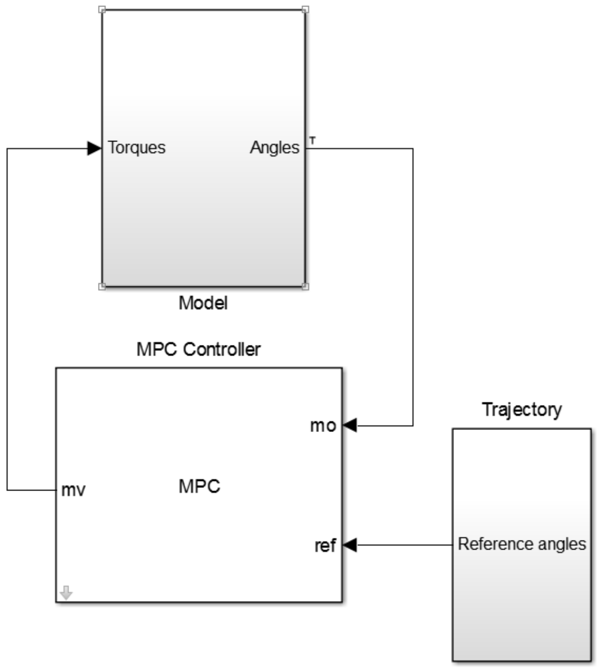

Figure 5.4: Working of MPC, Plant and Analytical block

In this chapter it describes the main MPC parameters that affect the management system:

First of all, it is needed to get internal model of MPC. The internal model defines character of management. Secondly, it is needed to determine what part of the objective function is more important to us and choose end-point or continuous decision. Thirdly, next important parameters are Constraints, which set values of maximum loads and extreme system positions. End at the end we need find how quickly and accurately our system must work. The first two parameters are determined by a logical explanation of their actions. The third parameter is from human biomechanics. The fourth parameter must be determined empirically. Also simplified scheme of full system presented in fig. (5.4).

6. SIMULATIONS AND RESULTS

Model of human gait, developed earlier must be tested on experimental data. In this chapter, the model is tested by simulating the human gait. The experimental data were obtained using a Vicon motion capture system in ITMO University. Fidelity model is determined by comparing the outputs of the kinetic modeling and reference experimental data. These basic results will be discussed later, to verify the possibility of forecasting models.

6.1. Required parameters

To simulate for MPC and analyzer requires mathematical model parameters, namely the length of the links, the moments of inertia, mass, center of mass, each link as well as the start and end step position. Mass units, moments of inertia, and the relative location of the centers of mass is calculated by the empirical equations [46], which depends on the total mass and human growth. The lengths of the links, the start and end positions are calculated using the program. For the mathematical model and the MPC models used one and same anthropometric parameters as MPC control parameters obtained by optimization model.

The formula for calculating the mass of the inertial body characteristics of men by weight (M) and a body length (H) looks like:

$$Y = B_0 + B_1 \cdot M + B_2 \cdot H \quad (5.5)$$

where Y – segment mass, B_0, B_1, B_2 are coefficients that are presented at table 5.1

Table 5.1 Coefficients of mass for eqn. (5.5)

Segment	B_0	B_1	B_2
Shin	−1.592	0.0362	0.0121
Hip	−2.649	0.1463	0.0137
Upper body	10.3304	0.60064	0.04256

For inertia moments coefficients are looks same and derived in [46]. However these equations are not suitable for women and children, also these equations can't be used for pathological patients, because their masses and inertia moment can be completely different. So for testing this system now, only suitable human gaits are gaits of healthy men's.

6.2. Results

6.2.1. Model 1

Modeling of human gait, succeeds with the parameters specified previously, fidelity model can be estimated by the model's ability to achieve the goal (end position), as well as by comparing the kinematic data and models obtained in the course of the experiment. And the final position and kinematic data captured using Vicon cameras, which makes it a fairly high accuracy for angular (sagittal) the position of each joint.

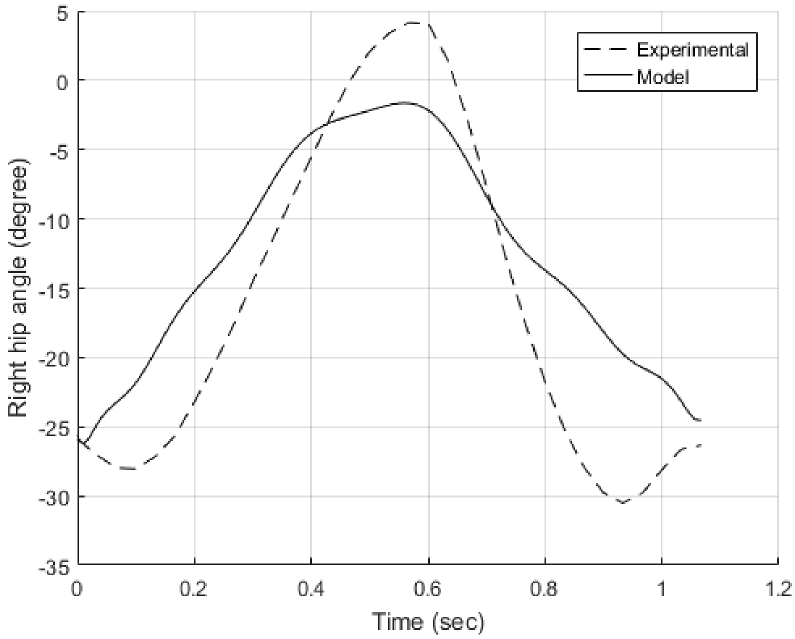

9

Figure 6.1: Sagital Plane Right Hip Angle (Simulation and Experimental)

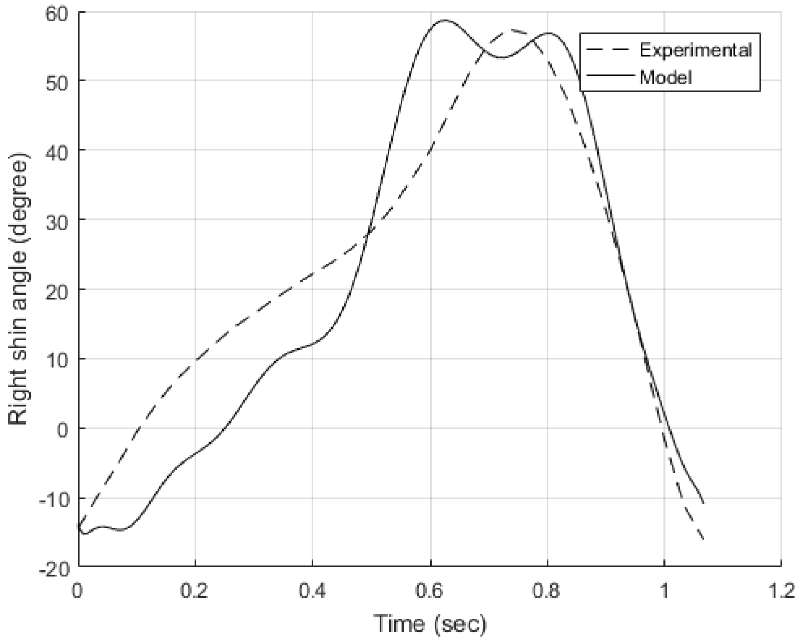

Figure 6.2: Sagital Plane Right Shin Angle (Simulation and Experimental)

In fig. 6.1 can be seen, that model angle doesn't reaches the desired value, and shin angle has two peaks, when must have only one. First mistake may be due to incorrect determination of ending of first movement phase. Second mistake is obtained, because analytical block set very big angle, that more than predefined constraint for this angle.

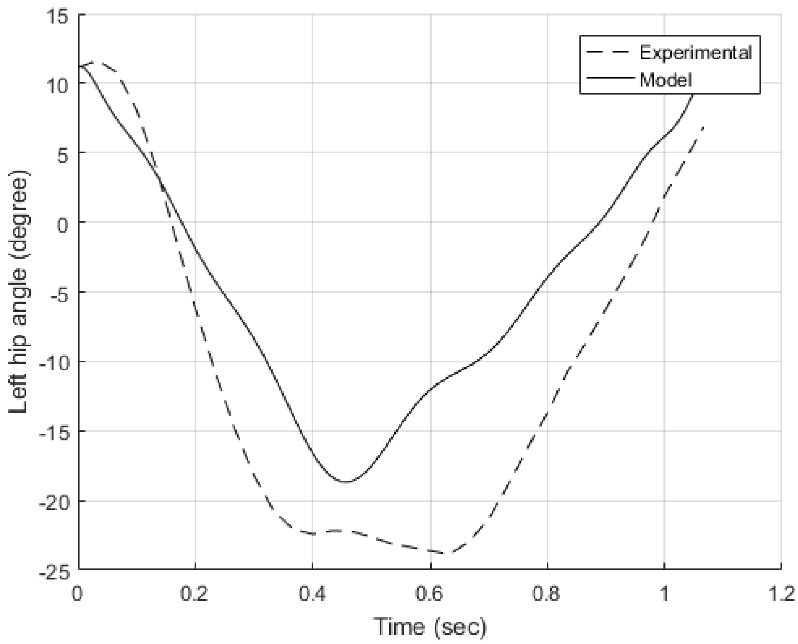

Figure 6.3: Sagital Plane Left Hip Angle (Simulation and Experimental)

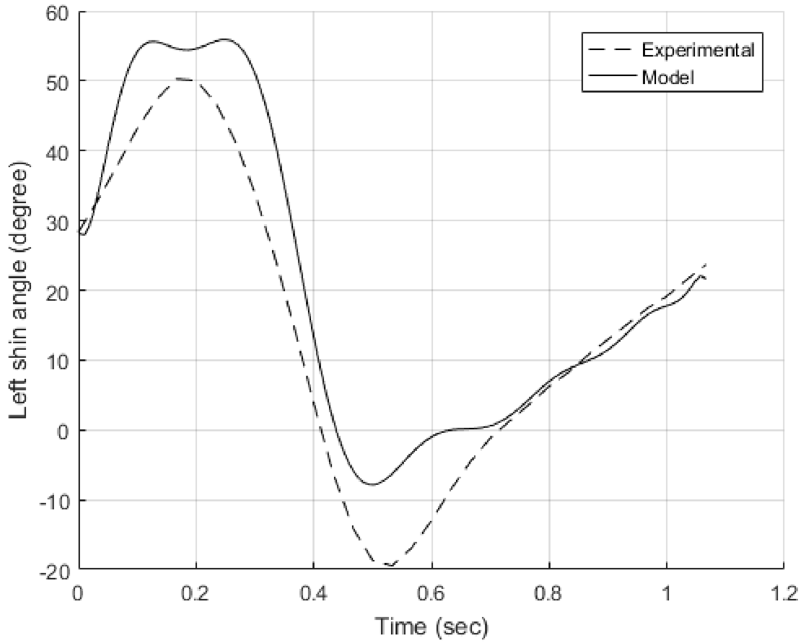

Figure 6.4: Sagital Plane Left Shin Angle (Simulation and Experimental)

Simulation of two full steps performed one after the other. Position at the end of the first step is used as the initial position for the second step. Kinematic simulation results are shown in fig. (6.1-6.4): The dotted line marked experimental data, solid line - simulation results. Each figure illustrates the value of the angle of the hips and legs to the vertical. To quantify the error between simulation results and experimental data, the mean square error (MSE) for the full step gait also calculated: To the right and left thighs are $6.2546° \ and \ 7.5277°$ right and left shins are $8.3327° \ and \ 7.9761°$.

6.2.2. Model 2

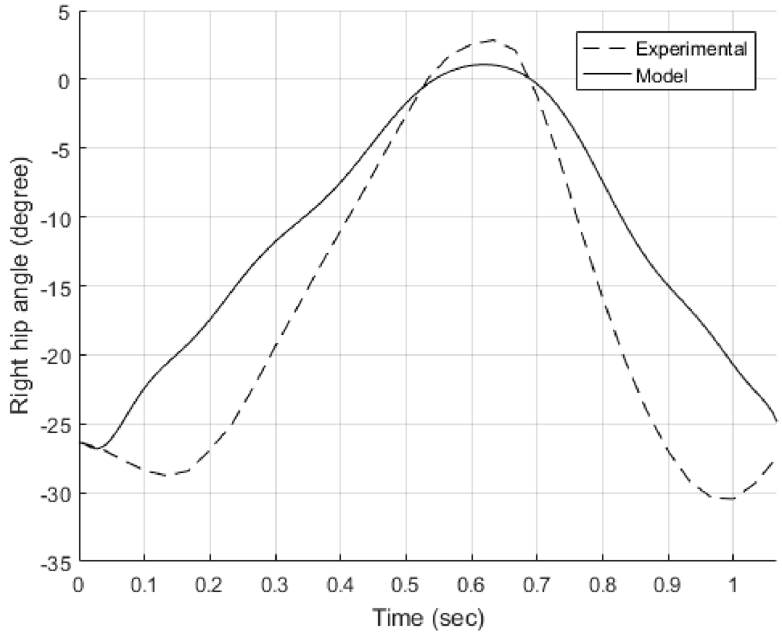

Figure 6.5: Sagital Plane Right Hip Angle (Simulation and Experimental)

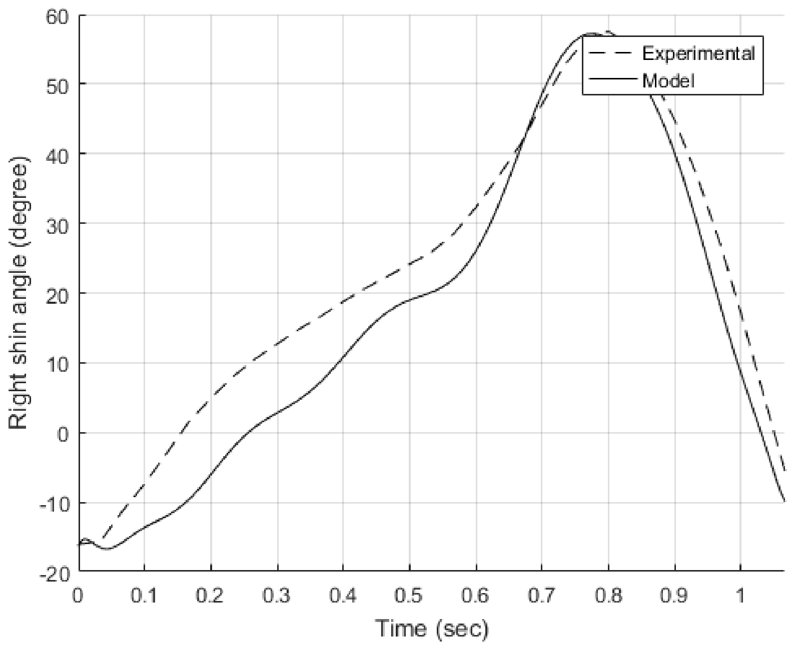

Figure 6.6: Sagital Plane Right Shin Angle (Simulation and Experimental)

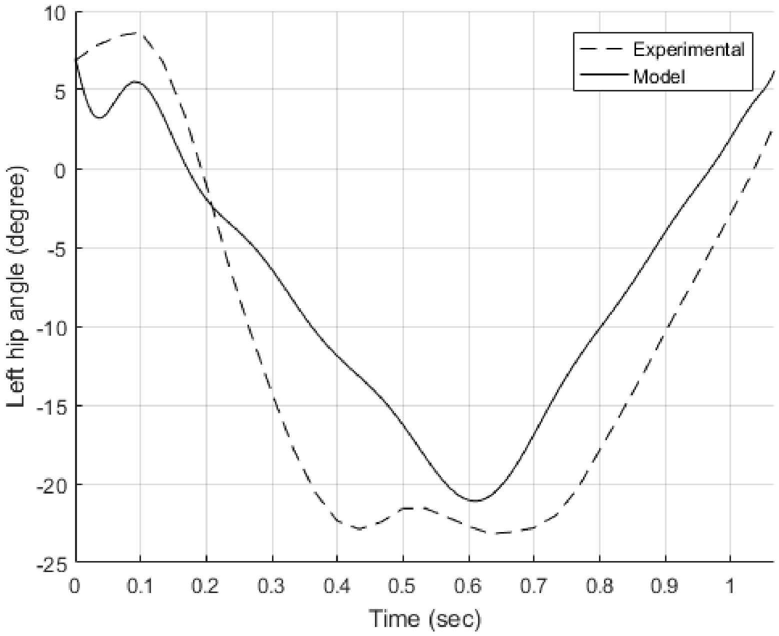

Figure 6.7: Sagital Plane Left Hip Angle (Simulation and Experimental)

If we compare the results obtained in the first movement and the second movement, that the experimental data are extremely weak, but the data of the same model vary greatly, and a second simulation is much closer to the ideal than the first. This difference is due to the strong dependence of the controller and the analysis unit of the given initial and final data for the entire step as a whole they are slightly different, because precise repeatability of movement going on to step right and then the left foot, but interim results may differ from step to step. This difference is expressed in the body at the reference position, the left foot, as well as in the time interval of status. From this it follows that an intermediate position in which the status has changed is output foot more closely in the future.

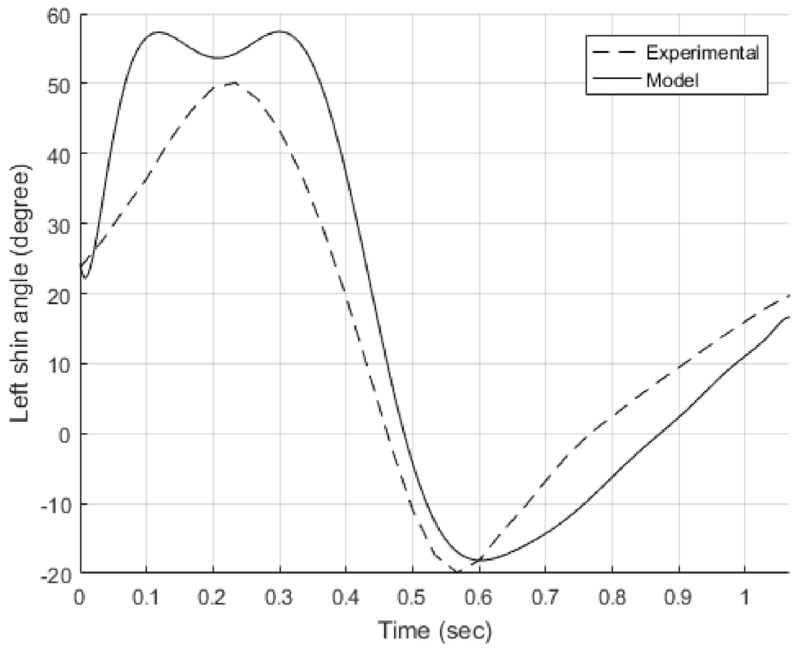

Figure 6.8: Sagital Plane Left Shin Angle (Simulation and Experimental)

Simulation of two full steps performed one after the other. Position at the end of the first step is used as the initial position for the second step. Kinematic simulation results are shown in fig. (6.1-6.4): The dotted line marked experimental data, solid line - simulation results. Each figure illustrates the value of the angle of the hips and legs to the vertical. To quantify the error between simulation results and experimental data, the mean square error (MSE) for the full step gait also calculated: To the right and left thighs are $6.8226° \; and \; 6.6601°$ right and left shins are $5.95° \; and \; 10.145°$.

6.3. Discussion of Simulation Results

The model developed in the first predictive model is focused on achieving the goal (end angle), regardless of the kinematic trajectory, so it is assumed that the model must first reach the end point, but the model is also good to predict the kinematics of human motion in the sagittal plane error to 8.5°.

Externally movement anthropomorphic model obtained angles dynamics as a whole follows the human movement. The fundamental error in the movement of the model is shown in the interval 0.38-0.62 seconds, characteristically seen in Fig. []. This error is caused by the fact that the movement of the model is divided into two intervals in which the right leg is the supporting or not, although there is a gap in the movement when both feet are supporting (double support phase). As a result, the period during the single support phase admixed by two phase reference, which affects the error in the form of provisions for the support legs, despite the fact that the support leg movement kinematics in times easier tolerated. It should be noted that the most difficult part of the movement is precisely the rise of portable legs immediately after repulsion.

7. SUMMARY AND FUTURE WORK

In this research we developed a model of human movement using prediction. The developed model includes a mathematical model of human gait, the model function as the control object and a control system in the form MPC, CNS mimics.

The effectiveness of the developed model is verified by simulation and comparison of the data with the experimental data. The simulation results showed that the model is able to predict the movement kinematics of a healthy person.

MPC management goals are achieved accurately and kinematic data models behave, as well as experimental, but the kinematics is not entirely consistent on the central segment of movement (double support phase). The discrepancies can be caused by several reasons: First, it is that the model is highly simplified representation of the human body. The second - in the sagittal plane of the units of length in man will be constantly changing, as rotation occurs not only in the sagittal plane but also in the frontal and longitudinal planes. The third is that, strictly speaking, human movement must be considered in three separate intervals - singly, two-supporting and single support on the other foot, otherwise the inevitable errors of the non-equivalence of support in the two reference phase (only one point of time the body will draw about the same in both) of the support.

This work is not the end of the research topic. The aim of this work was to develop a simple model of human gait, based on predictive control method, as well as in the previous task approximate trajectory analytically. The main part of this work is the use of the theory of motion of anthropomorphic mechanisms with impulse control and the use of predictive control method for modeling of human gait.

According to the author, the central nervous system uses a predictive control method, instead of the more common in classical control engineering feedback, and also the central nervous system, in addition to the predictive method using analytically derived or familiar (learned) a motion path that the system tries to repeat. This method of utilizing MPC and analytic trajectories may be to be used as the basic idea of the future work. In addition, this simulation method can be used in the study of the fundamental differences of different gaits of people, the diagnosis of diseases (differences from potentially healthy counterpart). And also, this method can be used in this form for autonomous imaging of human gait, as deviation of 8.5°, almost negligible in this video imaging gait.

The same principle had been respected simple and easy structure of the internal model, which allows a complement / complicate the model to approximate it to the real and reduce the prediction error.

KOKKUVÕTE

Selles uurimistöös käsitletakse mudel, mis simuleerib inimeste kõndimist MPC kasutades. Arenenud mudel koosneb, inimeste kõndimiste matemaatilise mudelist, juhtimise funktsioonist ja MPC juhtimis süsteemist, mis simuleerib CNS (kesk närvi süsteem).

Arenduse mudeli effektiivsus kontrollitakse modeleerimise ja eksperimendist saanud andmetega võrdlemise abil. Mudeleerimise tulemused näidisid, et mudel võib ennustada tervist inimest kinemaatikat.

MPC juhtimise eesmärgid saavutatakse suure täpsusega, ja mudeli kinemaatika andmed käituvad enda nagu eksperimentaalsed, aga kesk liikumise punktis kinemaatika mitte täielikult vastab reaalsust. Erinevusele võib olla mitu põhjust: esimiseks, mudel on liiga lihtsustatud, teiseks, sagitaalse lennukis reisi ja sääri projektsiooni pikkus, hakkab kogu aeg muutuma, sest pöörlemise toimub mitte ainult sagetaalses lunnukis, vaid frontaalses ja pikisuunalises linnukites. Kolmandaks, inimeste liikumine peab olema käsitletud kolmes erinevates intervaalitedes - ühetoetamise faas esimesele jalale, kahetoetuse ja ühetoetuse faas teise jalale. Muu juhul võivad tekkida vead, sest erinevad toetuse aste kahetoetuse faasis.

See töö ei ole uurimuse lõpp. Selle töö eesmärk on inimese kõndimis mudeli loomine, mis on ehitatud ennustamis juhtimis baasil ja eelmise analüütiliselt lähendatud ülesannel. Selle töö põhi osa on antropomorfse mehanismide impulsiivse juhtimisega liikumise teooria kasutamine ja kõndimise ennustamise juhtimismeetodi mudelit kasutamine.

Autori arvates, kesk närvilise süsteem kasutab ennustamis juhtimis meetodi PID meetodi asemel. Veel kesk närvilis süsteem kasutab analüütilised ja varem õppinud andmed. See MPC metood ja analüütilise trajektooride meetod võib kasutada tuleviku uurimistöös. Veel, see meetod võib kasutada kõndimis fundamentaalse uurimiseks, haiguste diagnosteerimiseks. Sama meetod võib kasutada kõndimis autonoomse visualiseerimiseks, sest 8.5 kraadi vahe ei ole nähtav kõndimis modeleerimises.

Lihtne sise mudeli struktuur oli täidetud, mis võimaldab mudelit täienduda ja komplitseerida, et väheneda ennustamis vigu.

REFERENCES

1. Gage J., Deluca P., Renshaw T. *Gait analysis: Principles and applications.* Journal of Bone and Joint Surgery — American Volume (1995), vol. 77. pp. 1607-1623.
2. McGeer *T. Dynamics and control of bipedal locomotion.* Journal of Theoretical Biology (1993), vol. 163, (3). pp. 277-314.
3. Vergallo P., Lay-Ekuakille A., Angelillo F., Gallo I., Trabacca A. *Accuracy improvement in gait analysis measurements: Kinematic modeling.* in Proc. IEEE Instrumentation and Measurement Technology Conference, Italy (2015). Art. no. 7151587. pp. 1987-1990.
4. Luengas L.A., Camargo E., Sanchez G. *Modeling and simulation of normal and hemiparetic gait.* Frontiers of Mechanical Engineering (2015) vol. 10 (3) pp. 233-241.
5. Gill T., Keller *J*.M., Anderson D.T., Luke R. *A system for change detection and human recognition in voxel space using the Microsoft Kinect sensor.* Applied Imagery Pattern Recognition Workshop (AIPR), (2011). pp. 1-8.
6. Sun J. *Dynamic Modeling of Human Gait Using a Model Predictive Control Approach.* PhD Dissertation Marquette University, (2015).
7. Ren L., Howard D., Kenney L. *Computational models to synthesize human walking.* Journal of Bionic Engineering (2006), vol. 3. pp. 127-138.
8. Ren L., Jones R., Howard D. *Predictive Modelling of Human Walking over a Complete Gait Cycle.* Journal of Biomechanics (2007), vol. 40 (7), pp. 1567–1574.
9. *M. Formalsky, Relocation of anthropomorphous mechanisms,* Principal edition of physical and mathematical literature (1982), (in Russian).
10. Tertychny-Dauri V. Y. Dynamics of robotic systems. Manual. ITMO, (2012), 128 pages, *(in Russian).*
11. Pontzer *H., Holloway J.H., Raichlen D.A., Lieberman D.E. Control and function of arm swing in human walking and running.* Journal of Experimental Biology (2009), vol. 212. pp. 523-534.
12. Marcus G. Pandy and Thomas P. Andriacchi. *Muscle and Joint Function in Human Locomotion.* Annual Review of Biomedical Engineering (2010), vol. 12: 401-433
13. Shuuji Kajita, Osamu Matsumoto, and Muneharu Saigo. *Real-time 3d walking pattern generation for biped robot with telescopic legs.* In Proceedings of the IEEE International Conference on Robotics and Automation, pages 2299–2306, Seoul, Korea, May 2001
14. *S*huuji Kajita, Fumio Kanehiro, Kenji Kaneko, Kiyoshi Fujiwara, Kazuhito Yokoi, and Hirohisa Hirukawa. *A realtime pattern generator for biped walking.* In Proceedings of 2002 IEEE International Conference on Robotics and Automation, pages 31–37, Washington, D.C., May 2002.
15. Shunsuke Kudoh and Taku Komura. *C2 continuous gait-pattern generation for biped robots.* In Proceedings of 2003 IEEE International conference on Intelligent Robots and Systems, pages 1135–1140, Las Vegas, NV, 2002.
16. Amos Albert and Wilfried Gerth. *Analytic path planning algorithms for bipedal robots without a trunk.* Journal of Intelligent and Robotic Systems, 36(2):109–127, February 2003.

17. Taesin Ha and Chong-ho Choi. *An effective trajectory generation method for bipedal walking.* Robotics and Autonomous Systems, 55(10):795–810, June 2007.
18. Tad McGeer. *Passive dynamic walking.* The International Journal of Robotics Research, 9(2):62–82, April 1990.
19. Yildirim Hurmuzlu, Frank Genot, and Bernard Brogliato. *Modeling, stability and control of biped robots a general framework.* Automatica, 40(10), October 2004
20. Arthur D. Kuo. *Stabilization of lateral motion in passive dynamic walking.* International Journal of Robotics Research, 18(9):917–930, September 1999
21. Steve Collins, Andy Ruina, Russ Tedrake, and Martijn Wisse. *Efficient bipedal robots based on passive-dynamic walker.* Science, 307(5712), February 2005
22. Arthur D. Kuo. *A simple model of bipedal walking predicts the preferred speed-step length relationship.* Journal of Biomechanical Engineering, 123(3):264–269, June 2001.
23. Arthur D. Kuo. *Energetics of actively powered locomotion using the simplest walking model. Journal of Biomechanical Engineering, 124(1):113–120, February 2002*
24. Arthur D. Kuo, J. Maxwell Donelan, and Andy Ruina. *Energetic consequences of walking like an inverted pendulum: Step-to-step transitions.* Exercise and Sport Sciences Reviews, 33(2):88–97, April 2005..
25.] A. Takanishi, M. Ishida, Y. Yamazaki, and I. Kato. *The realization of dynamic walking by biped walking robot wl40rd.* In Proceedings of the 1985 International Conference on Advanced Robotics, pages 459–466, 1985.
26. Jin-ichi Yamaguchi, Atsuo Takanishi, and Ichiro Kato. *Development of a biped walking robot compensating for three-axis moment by trunk motion.* In Proceedings of the 1993 IEEE/RSJ International Conference on Intelligent Robots and Systems, pages 561–566, Yokohama, Japan, July 1993.
27. J. Furusho and A. Sano. *Sensor-based control of a 9-link biped. I*nternational Journal of Robotics Research, 9(2):83–98, April 1990.
28. Hirofumi Miura and Isao Shimoyama. *Dynamic walk of a biped. I*nternational Journal of Robotics Research, 3(2):60–74, June 1984.
29. Kazuo Hirai. *The Honda humanoid robot: Development and future perspective.* Industrial Robot: An International Journal, 26(4):260–266, 1999.
30. Ching-long Shih. *The dynamics and control of a biped walking robot with seven degrees of freedom.* Journal of Dynamic Systems, Measurement and Control, 118(4):683–690, December 1996.
31. Yujiang Xiang, Jasbir Arora, and Karim Abdel-Malek. *Physics-based modeling and simulation of human walking: a review of optimization-based and other approaches.* Structural and Multidisciplinary Optimization, 42(1):1–23, July 2010.
32. Guy Bessonnet, P. Seguin, and Philippe Sardain. *A parametric optimization approach to walking pattern synthesis.* International Journal of Robotics Research, 24(7):523–536, July 2005.
33. Frank C. Anderson and Marcus G. Pandy. *Dynamic optimization of human walking. Journal of Biomechanical Engineering, 123(5):381–390, October 2001.*
34. R.T. Marler and J.S. Arora. *Survey of multi-objective optimization methods for engineering.* Structural and Multidisciplinary Optimization, 26(6):369–395, March 2004.
35. Herman van der Kooij, Ron Jacobs, Bart Koopman, and Frans van der Helm. *An alternative approach to synthesizing bipedal walking.* Biological Cybernetics, 88(1):46–59, January 2003.
36. Lei Ren, Richard K. Jones, and David Howard. *Predictive modeling of human walking over a complete gait cycle.* Journal of Biomechanics, 40(7):1567–1574, 2007

37. Peter Gawthrop, Ian Loram, and Martin Lakie. *Predictive feedback in human simulated pendulum balancing.* Biological Cybernetics, 101(2):131–146, July 2009.
38. M. Karimian, F. Towhidkhah, and M. Rostami. *Application of model predictive impedance control in analysis of human walking on rough terrains.* International Journal of Applied Electromagnetics and Mechanics, 24(3):147–162, 2005.
39. Filimonov YM *On the problem of optimal control mathematical pendulum* Differential equations 1965, t 1, M:. 8, p. 1007-1015.
40. Fomin SV, Shtilkind TI, *On the concept of equilibrium systems equipped legs.* Biophysics, 1972, t. 17, no. 1, p. 131-134.
41. Formal'skii AM, *Movement anthropomorphic mechanism under pulse upravlenii.- Proc .: Some problems of mechanics, robots and biomechanics.* M .: Univ. University Press, 1978, p. 17-34.
42. *Beletsky VV, Kirsanova TS, Flat linear models bipedal gait-* Math. AN SSSR, MTT, 1976, No. 4, p. 51-62.
43. Beletsky VV, Kirsanova TS, PS Chudinov, *walking Management and dynamics of systems, in dvuiogih .:* Biomechanics. Riga, 1975, p. 627-631.
44. Shilov GE*, Introduction to the theory of linear spaces* .-- M .: Gostskhizdat, 1956.- 304 p.
45. Sainburg Robert L. *Convergent Models of Handedness and Brain Lateralization, Frontiers in Psychology (2014), vol.5*
46. Dubrovsky VI, Fedorov VN*, Biomechanics: A textbook for secondary and higher education,* Moscow (2004) VLADOS PRESS - 672 pages
47. Sun, Jinming, "*Dynamic Modeling of Human Gait Using a Model Predictive Control Approach*" (2015). Dissertations (2009 -). Paper 526.

APPENDENCES

Appendix A. Control System MATLAB Code

This appendix shows the control program source code developed using MATLAB

```
clc;
clear;
%Obtain initial and end-point positions, and experimental data from bvh
%file
aa=82;
bb=64;
bb2=aa;
aa2=96;
%32 46 64
[angles,lengthes,time,height,points]=motioncap(aa);
%Load predefined MPC parameters
load MPCF2.mat
%Initial XY position of model
LPX=0;
LPY=0;
%Write angles for first motion
for nn = 1:5
for ff=bb:aa
angles2(nn).angle(ff-bb+1)=angles(nn).angle(ff);
time2(ff-bb+1)=time(ff);
end
end
time2=time2-time(bb);
% Define mass and inertias
for hh=1:1
M=69+hh;
ms=-0.8290+0.0077*M+0.0073*height;
mb=-1.5920+0.0362*M+0.0121*height;
ma=-2.6490+0.1463*M+0.0137*height;
mk= M-2*(mb+ma+ms);
mb2=M*0.05;
mb3=M*0.02;

ls=0.0385*height/100;
Lb=0.2844*height/100-ls;
La=0.5208*height/100-Lb-ls;

b=Lb-(-6.05-0.0390*M+0.142*height)/100;
a=La-(-2.420+0.0380*M+0.1350*height)/100;
r=0.7415*height/100-0.5208*height/100;

Kb=mb*b;
Kr=mk*r;
Ka=ma*a+mb*La;

Jab=Kb*La;

Joa=(-1152+4.594*M+6.815*height)/10000+ma*a^2;
Ja=Joa+mb*La^2;
Jb=(-3690+32.020*M+19.240*height)/10000+mb*b^2;
jj=(367+18.3*M-5.73*height)/10000;
```

```
J=mk*r^2;

O1=angles2(2).angle(1);
O2=angles2(3).angle(1);
I1=angles2(4).angle(1);
I2=angles2(5).angle(1);
fi=angles2(1).angle(1);
%
O1T=angles2(2).angle(aa-bb+1);
O2T=angles2(3).angle(aa-bb+1);
I1T=angles2(4).angle(aa-bb+1);
I2T=angles2(5).angle(aa-bb+1);
fiT=angles2(1).angle(aa-bb+1);
% Define Mathematical model
B=[J La*Kr 0 Lb*Kr 0
        La*Kr Ja-2*La*Ka+M*La^2 -La*Ka Jab-La*Kb-Lb*Ka+La*Lb*M -La*Kb
        0  -La*Ka Ja -Lb*Ka Jab
        Lb*Kr Jab-La*Kb-Lb*Ka+La*Lb*M -Lb*Ka Jb-2*Lb*Kb+Lb^2*M -Lb*Kb
        0  -La*Kb Jab -Lb*Kb Jb];

    A=[-Kr  0       0  0       0
        0   Ka-La*M 0  0       0
        0   0       Ka 0       0
        0   0       0  Kb-Lb*M 0
        0   0       0  0       Kb];
    g=9.81;
    [S,D1] = eig(g*inv(B)*A);
    R=S;
    D=[D1(1,1)
        D1(2,2)
        D1(3,3)
        D1(4,4)
        D1(5,5)];
    ww=sqrt(abs(D));

    tau=time2(length(time2))-time2(1);
    T=time2(length(time2))-time2(1);

    TT=0;
% write initial and end positions for Simulink
    z0=[fi O1 O2 I1 I2]';
    x0=R^(-1)*[fi O1 O2 I1 I2]';
    xT=R^(-1)*[fiT O1T O2T I1T I2T]';
    z01=[fi O1 O2 I1 I2]';
    zT=[O1T O2T fiT I1T I2T]';
% Simulate first step
sim 'onesup7linknew223.slx'
%Write start XY position for next step
LPX=LastPoint(length(LastPoint(:,1)),1);
LPY=LastPoint(length(LastPoint(:,1)),2);;
end
ll=length(Datafor2(:,2));
for nn=1:(length(Datafor2(:,2))-1)
   DATA(nn,:)=Datafor2(nn,:);
end

% Same process for left length
[angles3,lengthes3,time3,height3,points3]=motioncap(aa2);

for nn = 1:5
```

```
for ff=bb2:aa2
angles4(nn).angle(ff-bb2+1)=angles3(nn).angle(ff);
time4(ff-bb2+1)=time3(ff);
end
end

O1=Datafor2(length(Datafor2(:,2)),5);
O2=Datafor2(length(Datafor2(:,2)),6);
I1=Datafor2(length(Datafor2(:,2)),2);
I2=Datafor2(length(Datafor2(:,2)),3);
fi=Datafor2(length(Datafor2(:,2)),4);
O1T=angles2(4).angle(1);
O2T=angles2(5).angle(1);
I1T=angles2(2).angle(1);
I2T=angles2(3).angle(1);
fiT=angles2(1).angle(1);

    T=time4(length(time4))-time4(1);

    z0=[fi O1 O2 I1 I2]';
    x0=R^(-1)*[fi O1 O2 I1 I2]';
    xT=R^(-1)*[fiT O1T O2T I1T I2T]';
    z01=[fi O1 O2 I1 I2]';
    zT=[O1T O2T fiT I1T I2T]';
sim 'onesup7linknew2232.slx'

% For Figures
       for nn = 1:6
Datafor5(:,nn)=Datafor2(:,nn);
Datafor4(:,2)=Datafor2(:,4);
Datafor4(:,3)=Datafor2(:,5);
Datafor4(:,4)=Datafor2(:,6);
Datafor4(:,5)=Datafor2(:,2);
Datafor4(:,6)=Datafor2(:,3);
       end

for nn=(ll):(length(Datafor2(:,2))+ll-1)
    DATA(nn,:)=Datafor5(nn-ll+1,:);
    DATA(nn,1)=DATA(ll-1,1)+Datafor5(nn-ll+1,1);
end


for nn = 1:5
for ff=bb:aa2

angles5(nn).angle(ff-bb+1)=angles3(nn).angle(ff);
time5(ff-bb+1)=time3(ff)-time3(bb);
end
end
angles6(1).angle=angles5(2).angle;
angles6(2).angle=angles5(3).angle;
angles6(3).angle=angles5(1).angle;
angles6(4).angle=angles5(4).angle;
angles6(5).angle=angles5(5).angle;

for nn = 1:5

        y=DATA(:,nn+1)';
        x=DATA(:,1)';
```

```
        p = polyfit(x, y, 15);
        f = polyval(p, x);
        FF(nn,:)=f;
        fsko=polyval(p,time5);

       for ii=1:length(fsko)
       QS(nn,ii)=(fsko(ii)*180/pi-angles6(nn).angle(ii)*180/pi)^2;
       end
       QSM(nn)=sqrt(sum(QS(nn,:))/ii);

end

h = figure(1); clf; hold on; grid on
xlim([0 time5(length(time5))])
xlabel('Time (sec)')
ylabel('Right hip angle (degree)')
plot(time5,angles6(1).angle*180/pi,'k--',x,FF(1,:)*180/pi,'k-')
legend('Experimental','Model','NorthEastOutside')

h = figure(2); clf; hold on; grid on
xlim([0 time5(length(time5))])
xlabel('Time (sec)')
ylabel('Right shin angle (degree)')
plot(time5,angles6(2).angle*180/pi,'k--',x,FF(2,:)*180/pi,'k-')
legend('Experimental','Model','NorthEastOutside')

h = figure(3); clf; hold on; grid on
xlim([0 time5(length(time5))])
xlabel('Time (sec)')
ylabel('Left hip angle (degree)')
plot(time5,angles6(4).angle*180/pi,'k--',x,FF(4,:)*180/pi,'k-')
legend('Experimental','Model','NorthEastOutside')

h = figure(4); clf; hold on; grid on
xlim([0 time5(length(time5))])
xlabel('Time (sec)')
ylabel('Left shin angle (degree)')
plot(time5,angles6(5).angle*180/pi,'k--',x,FF(5,:)*180/pi,'k-')
legend('Experimental','Model','NorthEastOutside')

h = figure(5); clf; hold on; grid on
xlim([0 time5(length(time5))])
xlabel('Time (sec)')
ylabel('Right hip angle (degree)')
plot(time2,angles2(2).angle*180/pi,MathData(:,1),MathData(:,3)*180/pi,'k-')
legend('Experimental','Model','NorthEastOutside')
%
h = figure(6); clf; hold on; grid on
xlim([0 time5(length(time5))])
xlabel('Time (sec)')
ylabel('Right shin angle (degree)')
plot(time2,angles2(3).angle*180/pi,MathData(:,1),MathData(:,4)*180/pi,'k-')
legend('Experimental','Model','NorthEastOutside')
%
h = figure(7); clf; hold on; grid on
xlim([0 time5(length(time5))])
xlabel('Time (sec)')
ylabel('Left hip angle (degree)')
plot(time2,angles2(4).angle*180/pi,MathData(:,1),MathData(:,5)*180/pi,'k-')
legend('Experimental','Model','NorthEastOutside')
```

```
h = figure(8); clf; hold on; grid on
xlim([0 time5(length(time5))])
xlabel('Time (sec)')
ylabel('Left shin angle (degree)')
plot(time2,angles2(5).angle*180/pi,MathData(:,1),MathData(:,6)*180/pi,'k-')
legend('Experimental','Model','NorthEastOutside')
```